Pontifícia Universidade Católica do Rio Grande do Sul
Faculdade de Biociências
Programa de Pós-Graduação em Biologia Celular e Molecular

Dissertação de Mestrado

DIANA CAROLINA ROSTIROLLA

Uridina monofosfato quinase (EC 2.7.4.22) de *Mycobacterium tuberculosis* como alvo para o desenvolvimento de drogas

Porto Alegre
2010

DIANA CAROLINA ROSTIROLLA

Uridina monofosfato quinase (EC 2.7.4.22) de *Mycobacterium tuberculosis* como alvo para o desenvolvimento de drogas

Dissertação apresentada como requisito para a obtenção do grau de Mestre pelo programa de Pós-Graduação em Biologia Celular e Molecular da Pontifícia Universidade Católica do Rio Grande do Sul.

Orientador: Diógenes Santiago Santos

Co-orientador: Luiz Augusto Basso

Porto Alegre
2010

DIANA CAROLINA ROSTIROLLA

Uridina monofosfato quinase (EC 2.7.4.22) de *Mycobacterium tuberculosis* como alvo para o desenvolvimento de drogas

Dissertação apresentada como requisito para a obtenção do grau de Mestre pelo programa de Pós-Graduação em Biologia Celular e Molecular da Pontifícia Universidade Católica do Rio Grande do Sul.

Aprovado em 10 de setembro de 2010.

Banca examinadora:

Maurício Reis Bogo

Mário Sérgio Palma

Diogo Onofre de Souza

AGRADECIMENTOS

Ao Prof. Diógenes Santiago Santos, agradeço pela oportunidade de desenvolvimento desse trabalho junto ao seu grupo de pesquisa e pelos ensinamentos proporcionados.

Ao Prof. Luiz Augusto Basso, agradeço pelo conhecimento compartilhado, pelas sugestões e correções do trabalho, bem como pelo estímulo durante todo o desenvolvimento do projeto.

Dedico um agradecimento especial à colaboradora e colega Ardala Breda, pelos ensinamentos que jamais serão esquecidos, pela paciência, pelas sugestões e dedicação a este trabalho, assim como pelo companheirismo durante esses dois anos de convivência.

Ao meu colega e hoje amigo, Leonardo Rosado, agradeço pela ajuda e conhecimento compartilhado durante os momentos de dificuldade deste trabalho, pelo otimismo e pelo tempo dedicado a finalização do projeto. Agradeço também pela amizade, pela compreensão e principalmente pelos momentos de descontração.

Aos meus colegas e amigos do CPBMF e da Quatro G, com os quais tive o prazer de compartilhar conhecimentos e que sempre se mostraram dispostos a ajudar na realização desse projeto. Agradeço pelos momentos de descontração, de amizade e companheirismo durante todo o tempo que passamos juntos.

Às minhas amigas e amigos, especialmente a Candida e a Amanda, que sempre estiveram presentes durante essa etapa da minha vida e que sem o carinho e compreensão, essa etapa não teria tanto valor.

Aos meus pais, Iolanda Rostirolla e Gelson Rostirolla, que mesmo longe sempre apoiaram minhas decisões. Agradeço pelos constantes ensinamentos, pelo estímulo e valores que serão para sempre importantes na minha vida.

Ao meu irmão Rafael Rostirolla, agradeço pelos ótimos momentos de convívio, pelo carinho e descontração.

SUMÁRIO

RESUMO

A Tuberculose (TB), causada pelo *Mycobacterium tuberculosis*, permanece entre as principais causas de morte por doenças infecto-contagiosas no mundo e estima-se que um terço da população mundial esteja infectada. A co-infecção com o HIV e a emergência de TB resistente a múltiplas drogas representam um desafio a saúde pública e tem estimulado a pesquisa por novos e mais efetivos agentes terapêuticos contra a doença. Os nucleotídeos pirimidínicos são moléculas essenciais em inúmeras reações bioquímicas e suas rotas de biossíntese são indispensáveis a progressão da TB. Nesse contexto, a proteína UMP quinase de *M. tuberculosis* (*Mt*UMPK), que catalisa a fosforilação de UMP a UDP, é um alvo promissor para o desenho racional de drogas anti-TB. Neste trabalho é reportado a clonagem da região codificante do gene *pyrH*, a expressão da proteína recombinante em *E. coli* e a purificação da enzima. Além disso, confirmaram-se a identidade e a atividade biológica da *Mt*UMPK. Cromatografia de exclusão por tamanho indicou que a proteína é um tetrâmero em solução e estudos cinéticos revelam um comportamento alostérico, sugerindo que a *Mt*UMPK participa na regulação de síntese de purinas *versus* pirimidinas. Experimentos através da técnica de calorimetria de titulação isotérmica (ITC) revelaram que o mecanismo cinético para os substratos é sequencial ordenado, onde a molécula de ATP liga-se na enzima livre, seguido da ligação do UMP, e que a liberação dos produtos ADP e UDP ocorre de forma aleatória.

Palavras-chave: Nucleotídeos pirimidínicos. Fosforilação. Drogas anti-TB. Gene *pyrH*. Comportamento alostérico. Tetrâmero.

ABSTRACT

Tuberculosis (TB) remains a leading infectious killer worldwide and its causative agent, *Mycobacterium tuberculosis*, infects one third of the world population. The HIV co-infection and the emergence of multidrug and extensively-resistant TB have provided a very alarming challenge to global health and led us to focus on the research for new and more effective therapeutics against the disease. Pyrimidine nucleotides are essential for many biochemical reactions and its synthesis constitutes an important step in the progression of TB. Therefore, the protein UMP kinase from *M. tuberculosis* (*Mt*UMPK), which catalyses the phosphorylation of UMP to UDP and does not resemble its eukaryotic counterparts, is a promising target for the rational antitubercular drug design. In the present work, we report cloning of the *pyrH* gene coding region, heterologous recombinant protein in *E. coli* and purification to homogeneity. Moreover, we confirmed *Mt*UMPK identity and its biological activity. Size exclusion chromatography showed that the protein is a tetramer in solution and kinetic studies revealed an allosteric behavior, suggesting that *Mt*UMPK participates in the regulation of purine *versus* pyrimidine biosynthesis. Isothermal titration calorimetry (ITC) experiments showed that catalysis proceeds by a sequential ordered mechanism, in which the UMP substrate binds to the enzyme after the addition of ATP molecule, followed by a random displacement of ADP and UDP products.

Keywords: Pyrimidine nucleotides. Phosphorylation. Antitubercular drug design. *pyrH* gene. Allosteric behavior. Oligomer.

1. INTRODUÇÃO

1.1 Tuberculose

A tuberculose (TB), causada principalmente pelo *Mycobacterium tuberculosis* (Mtb), é uma doença infecto-contagiosa com relatos já no Egito e Roma Antigos [1,2,3]. As primeiras lesões típicas da doença, encontradas em múmias egípcias e andinas como deformidades na espinha, datam de até 5 mil anos atrás [4]. A identificação de material genético de Mtb em tecidos de mamíferos primitivos sugere que a TB é uma doença antiga com ampla distribuição geográfica. A doença foi disseminada no Egito e Roma, existiu na América antes de Colombo e em Bornéu, antes de qualquer contato com o povo europeu. A presença de ácido desoxirribonucléico (DNA) da espécie *M. bovis*, que geralmente infecta animais, também foi encontrada em esqueletos humanos com evidências de TB, sugerindo que os animais com os quais a população estava em constante contato podem ter sido reservatórios para a infecção em humanos [2].

A epidemia de TB na Europa iniciou, provavelmente, no começo do século XVII e se estendeu pelos 200 anos seguintes. Cidades da Europa e da América do Norte, após a Revolução Industrial, proporcionavam um ambiente favorável à disseminação do patógeno por via aérea, uma vez que a densidade populacional era alta e as condições sanitárias precárias. Devido a este cenário, durante toda história, a TB foi a principal causa de morte nessas regiões [2,4]. A epidemia se disseminou lentamente para diferentes locais, incluindo a África, devido à exploração e colonização pelos Europeus e Norte-Americanos [2].

A falta de tratamento efetivo contra a doença levou Hermann Brehmer, em 1854, a criar o primeiro sanatório, com a crença de que uma alimentação saudável, exercícios e a altitude poderiam curar os pacientes internados que sofriam de TB. Esse modelo foi utilizado para a criação dos subseqüentes sanatórios, principalmente na Europa e Estados Unidos [2,4].

Apesar dos esforços de muitos estudiosos na definição dos sintomas e características, possíveis causas e formas de contágio da TB; apenas em 1882 o alemão Robert Koch (1843-1910) identificou o Mtb como o agente etiológico da TB. Trinta e nove anos depois, a vacina desenvolvida a partir da atenuação do bacilo

Calmette-Guérin (BCG) foi introduzida para uso em humanos, e tornou-se a principal estratégia profilática contra a TB [2,4].

Finalmente, a introdução de compostos anti-TB, como estreptomicina (1944) e isoniazida (INH) (1952) levaram a uma efetiva quimioterapia que reduziu drasticamente a mortalidade causada pela TB [4]. A posterior introdução de outras drogas, como a rifampicina (RIF) (1966) [5], pareceu fornecer um arsenal suficiente de agentes contra a doença. Com isso, em 1969, a U.S. Surgeon General afirmou que era hora de “fechar o livro para as doenças infecciosas” [4].

No entanto, a TB nunca foi erradicada e permanece entre as principais causas de morte por doenças infecciosas mundialmente, especialmente na Ásia e na África. Epidemiologistas estimam que 9,4 milhões de novos casos e 1,8 milhões de mortes causadas por TB ocorreram no ano de 2008, dos quais 1,4 milhões de casos (15% do total) e 0,5 milhões de mortos eram portadores do vírus da imunodeficiência humana (HIV). Nesse contexto, a TB é a principal causa de morte por doenças infecciosas causada por um único patógeno [6].

Países da Ásia e da África correspondem a 55% e 30% da incidência de TB no mundo, respectivamente, enquanto que na Região das Américas a incidência atinge menores proporções (3%). O Brasil encontra-se na lista dos 22 países onde ocorrem 80% dos casos estimados de TB no mundo. Os altos valores estimados, particularmente para países africanos devem-se, em parte, às taxas relativamente altas de co-infecção com o HIV [6].

Além disso, a tuberculose resistente a múltiplas drogas (TB-MDR), que surge principalmente como resultado da má administração do tratamento, é um problema crescente em muitos países do mundo e será abordada no item 1.4 [7].

1.2 Patogenia

A TB pode ser causada por outras espécies de micobactérias (*M. africanum* e *M. bovis*) [3,5], porém, o principal agente etiológico da doença em humanos é o Mtb, um microrganismo aeróbio e de crescimento lento. Embora esse patógeno possa infectar diversos órgãos do hospedeiro, a TB pulmonar é a manifestação mais comum [1,3,8].

A infecção é normalmente adquirida por inalação do bacilo [8-10] através de gotículas que são expelidas da garganta e dos pulmões de indivíduos que possuem a TB pulmonar ativa [1].

Embora a maioria dos bacilos inalada seja rapidamente destruída pelo sistema imune do hospedeiro, após atingir os pulmões a bactéria é geralmente fagocitada por macrófagos alveolares e condicionada a um estado de latência, uma vez que essas células são capazes de conter o crescimento, mas não de eliminar o patógeno. Em seguida, outras células do sistema imune são recrutadas e responsáveis pela resposta inflamatória gerada e pela formação do granulona, ou tubérculo, a principal característica da TB. Ao contrário da forma ativa, a TB latente não é contagiosa e, na maioria dos casos, os indivíduos infectados com o bacilo não desenvolvem a doença [3,8,10].

A TB ativa ocorre como resultado de uma nova infecção ou reativação da forma latente. A reativação da doença é frequentemente desencadeada por condições que comprometem o sistema imune do paciente tais como: casos de má nutrição, idade avançada, abuso de drogas, terapia com imunossupressores ou co-infecção com HIV [8-10]. A diminuição da resposta imune desencadeia uma série de eventos que podem levar ao rompimento do granuloma, danos ao tecido pulmonar e espalhamento de milhares de partículas infectadas através das vias aéreas [10].

Atualmente, a infecção por HIV representa o maior risco para o desenvolvimento da forma ativa da TB, estando essas doenças fortemente associadas, e sendo a TB a principal causa de morte devido a doenças infecciosas em pacientes portadores de HIV [3,6,9]. Casos de TB extrapulmonar, em particular a TB meningítica, também são mais comuns na população HIV positiva [9].

Indivíduos infectados com o bacilo, porém saudáveis, geralmente são assintomáticos. Os sintomas da TB pulmonar ativa se manifestam através da tosse, muitas vezes contendo escarro e sangue, dores do peito, fraqueza, perda de peso e sudorese noturna [2,4,9]. No entanto, após 2 a 4 semanas de tratamento apropriado, os sintomas diminuem, induzindo muitos pacientes a interromper a terapia [4].

1.3 Tratamento

Apesar de existirem diferentes regimes de tratamento contra a TB, a Organização Mundial da Saúde (OMS) recomenda aquele conhecido como DOTS (do inglês, *Directly Observed Treatment Short Course*) [3]. A quimioterapia consiste em uma associação de fármacos de primeira linha, INH, RIF, pirazinamida (PZA) e etambutol (EMB) durante dois meses, seguida por quatro meses com INH e RIF [4,7,11], podendo curar a maioria dos casos [4]. Além disso, a estratégia do DOTS inclui outros 5 componentes: i) estabelecer uma rede de indivíduos treinados a administrar e supervisionar o DOTS; ii) criar laboratórios e profissionais habilitados para o diagnóstico da TB; iii) implementar um sistema de fornecimento confiável de medicamentos de alta qualidade (preferencialmente, sem custo aos pacientes); iv) compromisso governamental e v) sistema de monitoramento dos casos, tratamento e resultados [2,7,12]. Essas estratégias previnem a ocorrência de novas infecções e, o mais importante, dificultam o surgimento de casos TB-MDR [3].

A falha do tratamento, definida como a presença de culturas positivas após cinco meses de terapia apropriada [6], pode ser resultado da falta de aderência pelo paciente devido à sua duração e complexidade, custo, possíveis efeitos adversos ou resistência do bacilo às drogas [9,11]. Tais circunstâncias favorecem o surgimento de organismos resistentes aos medicamentos utilizados no esquema terapêutico [4,11].

1.4 Resistência aos fármacos

Uma potencial ameaça ao controle da TB é a emergência de linhagens de Mtb que não podem ser contidas empregando-se as terapias padrões anti-TB [13].

As micobactérias possuem uma alta taxa de resistência intrínseca a maioria dos antibióticos e agentes quimioterápicos devido à difícil permeabilidade da sua parede celular. No entanto, tal barreira não tem capacidade suficiente para produzir níveis significativos de resistência, o que requer um mecanismo adicional [5].

A falta de adesão ao regime terapêutico pelo paciente, prescrição imprópria, dificuldade de acesso aos medicamentos e problemas farmacocinéticos são fatores

importantes para o surgimento de populações bacterianas resistentes a drogas altamente eficazes [9,14].

A TB-MDR é definida como aquela na qual o paciente possui a doença ativa com bacilo resistente a, pelo menos, INH e RIF. A TB-MDR pode ser contraída através de infecção com bacilos já resistentes (resistência primária) ou pode ser desenvolvida no decorrer do tratamento (resistência adquirida) [15]. Embora o DOTS seja altamente eficiente no controle da TB susceptível às drogas (ou resistente somente à INH), ele é comumente insuficiente no controle da TB-MDR [12,15]. Casos de TB-MDR são mais difíceis de curar e requerem um tratamento com drogas de segunda linha (fluoroquinolonas, aminoglicosídeos, tioamidas), as quais são menos efetivas e mais tóxicas, com exceção de algumas fluoroquinolonas, além de ter um custo mais elevado que os regimes baseados em medicamentos de primeira linha [12-16].

Dados baseados em pelo menos 100 países nos últimos 10 anos indicam que 5% do total de casos de TB são MDR (**Figura 1**). Em 2008, foi estimado pela OMS que 27 países responderam por 85% de todos os casos de TB-MDR. Entre eles, os cinco países que representam o maior número de casos são: Índia, Federação Russa, China, África do Sul e Bangladesh. Na América Latina, o Peru é o país que possui a maior porcentagem de casos de TB-MDR registrados (5,3%) entre os novos casos de infecção [15].

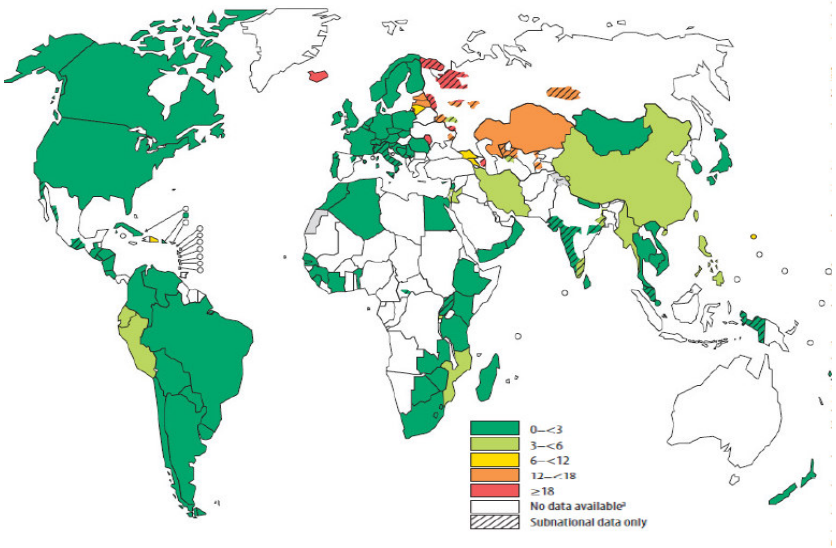

Figura 1. Índice global (%) de casos de TB-MDR entre novos casos de TB registrados desde 1994 [15].

Pacientes com TB-MDR e co-infectados com HIV são os que possuem o pior prognóstico, uma vez que essa associação tem provocado altas taxas de mortalidade, especialmente quando diagnosticada tardiamente [9,12].

Um estudo realizado por Kawai e colaboradores [17], no Peru, demonstrou um excelente prognóstico para indivíduos HIV negativos e uma rápida cura da infecção para pacientes com TB não MDR. No entanto, pacientes com TB-MDR tiveram um período de infecção prolongado e, aqueles co-infectados com HIV, morreram nos 2 primeiros meses de terapia (55%) [17].

Portanto, é evidente a necessidade de um rápido teste de suscetibilidade a drogas anti-TB em pacientes HIV positivos, melhora nas medidas de controle de infecção e tratamento precoce com terapia anti-retroviral para pacientes portadores de HIV e TB-MDR. Essas providências são essenciais para que os casos de TB-MDR sejam detectados e tratados adequadamente, reduzindo assim o risco de infecção e mortalidade [17,18].

Nos últimos anos, casos de TB extensivamente resistente às drogas (TB-XDR) têm sido relatados em diversos países. A definição mais recente para TB-XDR denota a condição em que os isolados são resistentes à INH e RIF, a alguma fluoroquinolona e a qualquer droga de segunda linha injetáveis (capreomicina, canamicina, amicacina), resultando em limitadas opções de tratamento [15].

Apesar das limitações dos testes laboratoriais para susceptibilidade às drogas de segunda linha, a maioria realizada apenas em isolados MDR, dados indicam que a TB-XDR está difundida em 58 países, com ao menos um caso reportado, e que 5,4% dos casos de TB-MDR são também XDR [15].

Indivíduos infectados com TB-XDR possuem um prognóstico ruim, com altos índices de falha do tratamento e alta mortalidade [12]. A situação torna-se ainda mais grave em pacientes portadores de HIV. Em um estudo realizado em uma área rural da África do Sul, a maioria dos pacientes (>90%) co-infectados com TB-XDR e HIV vieram a falecer, com uma média de sobrevivência de apenas 16 dias a partir do diagnóstico [19].

Recentemente, Velayati e colaboradores [20] documentaram o surgimento de novas formas de bacilos encontrados em pacientes diagnosticados com TB-MDR. Esses isolados foram classificados como linhagens totalmente resistentes às drogas (TDR), uma vez que apresentaram resistência *in vitro* a todas as drogas de primeira e segunda linha testadas. Durante o estudo, os pacientes infectados não

responderam a nenhuma terapia padrão e permaneceram com culturas positivas após 18 meses de tratamento com drogas de segunda linha [20].

Enquanto a TB-MDR e XDR significam uma ameaça à saúde pública e ao controle da TB no mundo, possíveis casos de TB-TDR aumentam a preocupação quanto a uma futura epidemia de TB incurável [20]. Diante de tal cenário, há uma urgente necessidade de pesquisa por novas drogas anti-TB, além da aprovação e uso das que estão em desenvolvimento [12].

1.5 Desenvolvimento de novas drogas anti-TB

O desenvolvimento de novas drogas para o tratamento da TB envolve mais desafios que a busca por agentes terapêuticos para outras doenças [21]. Existem três fatores básicos envolvidos: reduzir a duração total do tratamento, eficácia contra casos de TB-MDR e XDR e promover tratamento efetivo para casos de infecção latente [22,23].

No entanto, a complexa biologia do Mtb, que permite sua persistência no hospedeiro em um estado de dormência durante anos, torna difícil a identificação das rotas metabólicas envolvidas nesse processo, e que sejam essenciais à sobrevivência do microrganismo. Além disso, existe pouca informação disponível a respeito do metabolismo do patógeno durante esta fase e sobre os possíveis locais de infecção no hospedeiro [21,22].

A emergência de cepas MDR e XDR, bem como a epidemia de HIV levam a uma urgente necessidade de melhor entendimento sobre os mecanismos moleculares de ação e de resistência às drogas, facilitando a pesquisa por novos compostos anti-TB efetivos tanto no combate da TB susceptível às drogas quanto em casos MDR/XDR [3].

Tratamentos futuros requerem medicamentos com menos efeitos adversos a fim de facilitar a adesão à terapia. Esses novos agentes devem, idealmente, provocar o mínimo de interações farmacológicas com drogas anti-retrovirais comumente utilizadas para tratar pacientes co-infectados com HIV e, possivelmente, outras medicações [18]. Outro atributo, e de grande importância, é que novos compostos devem ser capazes de produzir um efeito bactericida contra o Mtb tanto

no estado de multiplicação ativa quanto no estado de dormência, a fim de combater toda população microbiana presente nos tecidos do hospedeiro [21].

2. METABOLISMO DE NUCLEOTÍDEOS

Os nucleotídeos são ésteres de fosfato de um açúcar de cinco átomos de carbono (pentose), nos quais uma base nitrogenada está covalentemente ligada ao C1´ do resíduo de açúcar (**Figura 2**). Os ribonucleotídeos constituem as unidades monoméricas do ácido ribonucléico (RNA), no qual a pentose é a D-ribose, enquanto que os desoxirribonucleotídeos possuem a desoxi-D-ribose como pentose e são as unidades monoméricas do DNA.

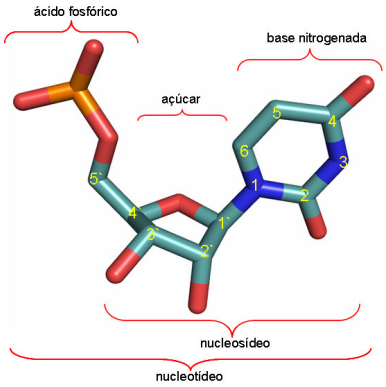

Figura 2. Estrutura de um nucleotídeo. A ligação glicosídica entre o açúcar e a base nitrogenada forma o nucleosídeo. Quando um ácido fosfórico é esterificado com um grupo hidroxila da porção açúcar de um nucleosídeo, forma-se um nucleotídeo. O nucleotídeo mostrado é a uridina 5´-monofosfato. Átomos de carbono em ciano, nitrogênio em azul, oxigênio em vermelho e fósforo em laranja. Os átomos de hidrogênio foram omitidos para maior clareza da figura. Numeração padrão dos átomos da base e do açúcar em amarelo.

As bases nitrogenadas são moléculas planas, aromáticas e heterocíclicas, derivadas de purinas ou pirimidinas. Os principais componentes purínicos dos ácidos nucléicos são os resíduos de adenina (A) e guanina (G); os resíduos pirimidínicos são os de citosina (C), uracila (U), que ocorrem principalmente no RNA, e timina (T), que ocorre no DNA [24].

Os nucleotídeos são compostos que participam de uma infinidade de processos bioquímicos e são classificados em purínicos e pirimidínicos. Eles atuam como fonte de energia em rotas metabólicas, participam na sinalização celular, na

regulação de rotas de biossíntese, além de exercerem outras inúmeras funções [24-26].

O metabolismo de nucleotídeos requer um controle fino, pois eles devem estar presentes em quantidades específicas e no momento correto para a síntese de ácidos nucléicos, permitindo a replicação celular e a síntese de proteínas, além de serem moléculas carregadas negativamente, cujos níveis devem ser controlados para manter o balanço eletroquímico das células [26].

Uma vez que a maioria dos ácidos nucléicos proveniente da dieta é metabolizada pelas células epiteliais do intestino, o aproveitamento de purinas e pirimidinas é mínimo; portanto ambas necessitam ser sintetizadas através da síntese *de novo*, ou a partir dos produtos de degradação dos ácidos nucléicos, pela via de salvamento de bases nitrogenadas [24,25].

2.1 Síntese *de novo* e via de salvamento de pirimidinas

Pirimidinas são moléculas onipresentes entre os reinos animal e vegetal, e as reações envolvidas na sua biossíntese são conservadas na maioria dos organismos [27].

As bases pirimidínicas podem ser sintetizadas tanto através da via *de novo*, a partir de glutamina e bicarbonato, quanto a partir de uracila pela via de salvamento de pirimidinas, originando uridina 5´-monofosfato (UMP), o qual é o precursor comum da formação de outros nucleotídeos pirimidínicos [25,27].

Síntese de novo

A síntese *de novo* de pirimidinas compreende seis reações bioquímicas e, diferente do que ocorre na síntese de bases púricas, o anel pirimidínico é sintetizado antes de ser ligado à molécula de ribose 5´-fosfato [24,25]. Como ilustrado na **Figura 3**, a formação do anel ocorre a partir de inúmeras reações bioquímicas que resultam na síntese de orotato [28]. Subsequentemente, a enzima orotato-fosforribosil-transferase (OPRT) catalisa a transferência da ribose 5´-fosfato do 5-fosforribosil-α-1´-pirofosfato (PRPP) para o orotato, originando o primeiro nucleotídeo pirimidínico, a orotidina 5´-monofosfato (OMP), que posteriormente sofre descarboxilação pela OMP-descarboxilase (ODCase) para formar UMP [24,25,27].

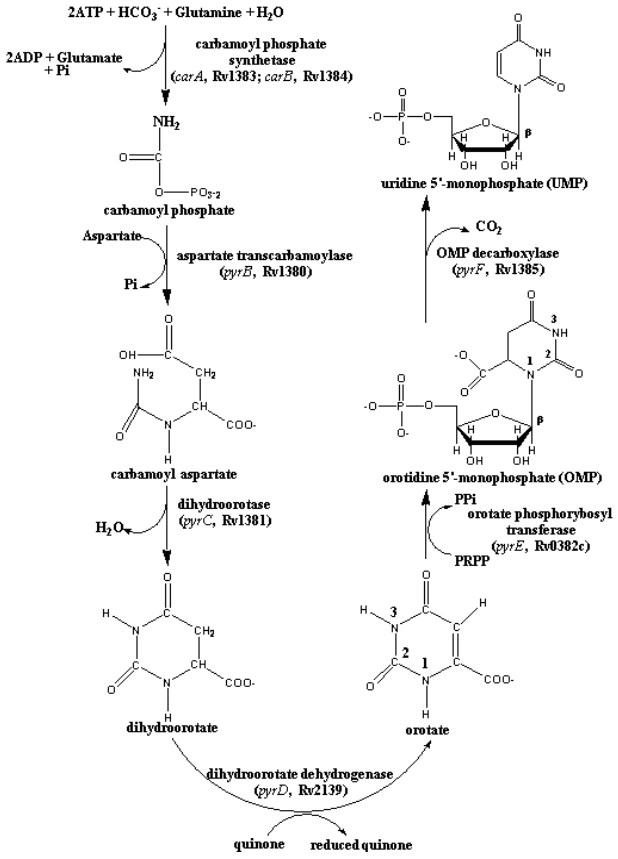

Figura 3. Rota metabólica da síntese *de novo* de UMP. Estão representadas na figura, as seis rotas catalisadas por enzimas, bem como os produtos formados a cada reação. Os genes que codificam cada enzima estão descritos entre parênteses.

Em bactérias, as seis atividades enzimáticas responsáveis pela biossíntese de UMP são catalisadas por proteínas independentes. No entanto, em animais, as primeiras três enzimas estão localizadas em uma única cadeia polipeptídica, denominada CAD, assim como as duas últimas enzimas da via (OPRT e ODCase), presentes em um polipeptídeo denominado UMP sintase [24,25,27].

A síntese de uridina 5´-trifosfato (UTP) ocorre a partir da fosforilação de UMP, a partir de sucessivas reações de uma enzima nucleosídeo monofosfato quinase e uma enzima nucleosídeo difosfato quinase. Para a síntese de citidina 5´-trifosfato (CTP) a partir de UTP, um grupo amina é adicionado ao carbono 4 da base nitrogenada pela enzima CTP-sintetase. UTP e CTP são precursores do RNA, já o dTMP, sintetizado a partir da desoxiuridina 5´-monofosfato (dUMP) pela enzima timidilato sintase (TS), está presente no DNA [24,25].

Via de salvamento

A via de salvamento de pirimidinas permite que os nucleotídeos pirimidínicos sejam sintetizados a partir de bases pirimidínicas livres e nucleosídeos provenientes da degradação de ácidos nucléicos, e requer uma demanda de energia menor que a rota de síntese *de novo* [26,28].

A via de salvamento de pirimidinas consiste em rotas de duas etapas: a primeira é a conversão de bases livres em seus respectivos nucleosídeos pelas fosforilases de nucleosídeos pirimídicos, que podem ser específicas para uridina (UP1 e UP2 – do inglês, *uridine phosphorylase*) ou para timidina (TP – do inglês, *thymidine phosphorylase*), como nos mamíferos, ou por fosforilases de nucleosídeos pirimídicos com afinidade tanto para uridina quanto timidina, como no caso de bactérias, sendo denominadas PyNP (do inglês, *pyrimidine nucleoside phosphorylase*). Na segunda etapa da via, nucleosídeo quinases específicas promovem a conversão dos nucleosídeos em nucleotídeos (**Figura 4**) [25].

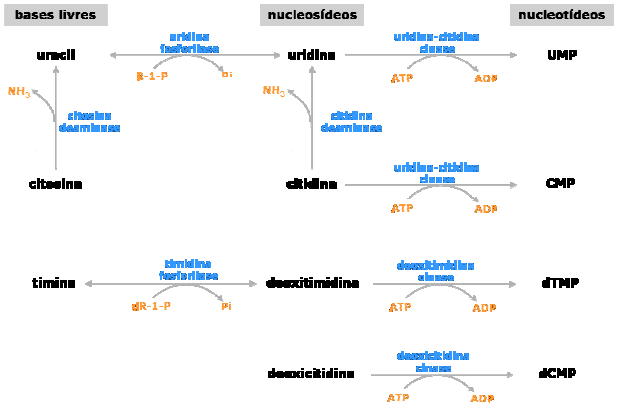

Figura 4. A via de salvamento de bases pirimídicas ocorre pela conversão de bases livres em seus respectivos nucleosídeos por pirimidina nucleosídeo fosforilases, seguida pela conversão dos nucleosídeos em nucleotídeos pela ação de nucleosídeo quinases específicas.

Como exemplo, a uracila proveniente da dieta ou da degradação de nucleotídeos é convertida a uridina, por uma uridina fosforilase, e será fosforilada a UMP por uma uridina quinase específica [27].

Em procariotos, a uracila intracelular também pode ser convertida diretamente a UMP pela ação da enzima uracil-fosforribosil-transferase (UPRTase). A citosina intracelular sofre rápida desaminação à uracila e amônia, pela enzima citosina deaminase. A uracila originada nessa reação é convertida a UMP pela UPRTase. UMP formado a partir de uracila e citosina via salvamento de pirimidinas é

convertido a UDP, UTP, e CTP a partir de reações de fosforilação, da mesma forma que ocorre na síntese *de novo* (**Figura 5**) [29].

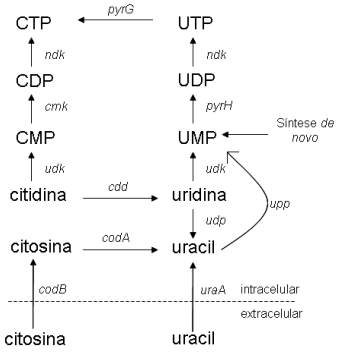

Figura 5. Rota de salvamento para uracila e citosina. O nome dos genes representa as proteínas codificadas correspondentes: *cdd*, citidina deaminase; *cmk*, CMP quinase; *codA*, citosina deaminase; *codB*, citosina permease; *udk*, uridina quinase; *udp*, uridina fosforilase; *upp*, UPRTase; e *uraA*, uracil permease. Adaptado de Turnbough, et al., 2008.

2.2 Síntese de desoxirribonucleotídeos

Desoxirribonucleotídeos são derivados dos seus ribonucleotídeos correspondentes através da redução do átomo de C2´ da D-ribose, formando 2´-desoxi-D-ribose [26]. A redução ocorre na molécula durante a etapa de dinucleotídeo e é catalisada por enzimas denominadas ribonucleotídeo-redutases (RNRs). A última etapa na produção de desoxirribonucleosídeos trifosfato (dNTPs) é a fosforilação dos respectivos desoxirribonucleosídeos difosfato (dNDPs), numa reação catalisada pela mesma enzima que fosforila NDPs [24,25].

Desoxiuridina 5´-difosfato (dUDP) pode ser desfosforilado a dUMP, ou, desoxicitidina 5´-monofosfato (dCMP) pode ser desaminado para formar dUMP. A formação de dTMP, como mencionado anteriormente, ocorre a partir do dUMP pela enzima TS. Reações subsequentes de fosforilação produzem desoxitimidina 5´-trifosfato (dTTP), um precursor da síntese de DNA [25].

3. NUCLEOSÍDEO MONOFOSFATO QUINASES NA SÍNTESE DE NUCLEOTÍDEOS PIRIMIDÍNICOS

Nucleosídeo monofosfato (NMP) quinases são enzimas essenciais na biossíntese e na reciclagem de nucleosídeos trifosfatados e, embora apresentem especificidade por nucleotídeos purínicos ou pirimidínicos particulares, mas não pelo açúcar (ribose ou desoxirribose), elas representam uma família de proteínas homólogas com propriedades estruturais e catalíticas semelhantes a adenilato quinases (EC 2.7.4.3) [30].

Estas enzimas catalisam a transferência reversível de um grupo fosfato a partir de um nucleosídeo trifosfato, geralmente ATP, para nucleosídeos monofosfato, como na reação: ATP + NMP ↔ ADP + NDP, na presença de um cátion divalente [31,32]. Sucessivamente, os nucleosídeos difosfato formados serão fosforilados, e eventualmente reduzidos, a nucleosídeos trifosfato, os quais são precursores do RNA, DNA e fosfolipídeos [31].

Entre as NMP quinases envolvidas na síntese de pirimidinas, estão as uridina monofosfato quinases (UMPK – do inglês, *uridine monophosphate kinase*) procarióticas e eucarióticas que apresentam diferenças estruturais e de afinidade por substrato, apesar de ambas serem responsáveis pela geração de nucleosídeos difosfato.

3.1 Uridina monofosfato quinases como alvos para o desenho de drogas

Em eucariotos, a fosforilação de UMP e CMP, durante a síntese de pirimidinas, é realizada por uma única proteína, denominada UMP/CMP quinase [30,33]. UMP/CMP quinases de *Saccharomyces cerevisiae* (código PDB: 1UKY) e *Dictyostelium discoides* (código PDB: 1UKE) são monômeros, cuja seqüência de aminoácidos é homóloga a adenilato quinase [32,34]. No entanto, bactérias possuem duas enzimas distintas e com diferentes especificidades para UMP e CMP [30].

A CMP quinase de *E. coli* (código PDB: 1CKE) é um monômero assim como a maioria das NMP quinases e, apesar da pouca similaridade com essas proteínas

em relação à estrutura primária, ela conserva a estrutura quartenária encontrada em adenilato quinases ou em UMP/CMP quinases eucarióticas [35].

No entanto, UMPKs bacterianas (EC 2.7.4.22), codificadas pelo gene *pyrH* e altamente conservadas entre bactérias, não apresentam similaridades na sequência de aminoácidos quando comparadas às eucarióticas e não se assemelham a nenhuma outra NMP quinase. Estudos com modelos moleculares sugerem que a UMPK de *Bacillus subtilis*, *E. coli* (código PDB: 2BNE) e *Pyrococcus furiosus* (código PDB: 2BRX) compartilham similaridades estruturais com asparto quinases, carbamato quinases e *N*-acetilglutamato quinases [36-39].

Além disso, enquanto a enzima eucariótica pode fosforilar eficientemente UMP e CMP [30,33], UMPKs da maioria dos procariotos possui uma alta especificidade por UMP [31,39].

Genes que codificam UMPKs têm sido identificados na maioria dos genomas bacterianos [36] e têm-se mostrado essenciais para o crescimento em ambas bactérias Gram-positiva (*Streptococcus pneumoniae*), e Gram-negativa (*E. coli*) [40-42]. No entanto, desde que o gene *pyrH* de *B. subtilis* mostrou-se não essencial à sobrevivência deste patógeno, considerações a respeito destas enzimas como potenciais alvos de drogas requerem estudos mais detalhados [43].

Estratégias baseadas na pesquisa por novos alvos para agentes antimicobacterianos envolvem a identificação de enzimas presentes em rotas bioquímicas essenciais e exclusivas à viabilidade do bacilo [44]. Nesse contexto, um estudo realizado por Robertson e colaboradores, sugere que o gene *pyrH* é essencial para o crescimento do Mtb, tornando a UMPK um alvo interessante para o desenvolvimento de novas drogas anti-TB [45].

3.2 Uridina monofostato quinase de *Mycobacterium tuberculosis* (*Mt*UMPK, EC 2.7.4.22)

A enzima *Mt*UMPK, assim como as UMPKs bacterianas é uma enzima envolvida na síntese de nucleotídeos pirimidínicos. Ela catalisa a transferência de um grupo fosfato a partir do ATP para a molécula de UMP, gerando UDP, a partir do qual todos outros nucleotídeos pirimidínicos podem ser sintetizados.

A *Mt*UMPK, de 261 aminoácidos, é codificada pelo gene *pyrH* (Rv2883c) e possui uma seqüência de 786 pares de base, de acordo com a notação do genoma de Mtb H37Rv [46].

Sua seqüência de aminoácidos apresenta similaridades com UMPKs de outros organismos já estudadas. Entre elas, está a UMPK de *B. subtilis* (NP_389533.2), *S. pneumoniae* (YP_816317.1) e *E. coli* (NP_414713.1) [47] com as quais apresenta, respectivamente, 56,60 %, 52,92% e 45,49% de identidade [48] (**Figura 6**). Com base nessas semelhanças, é possível inferir algumas características da *Mt*UMPK, tais como: características estruturais, sítios de ligação a substratos e regiões de controle alostérico.

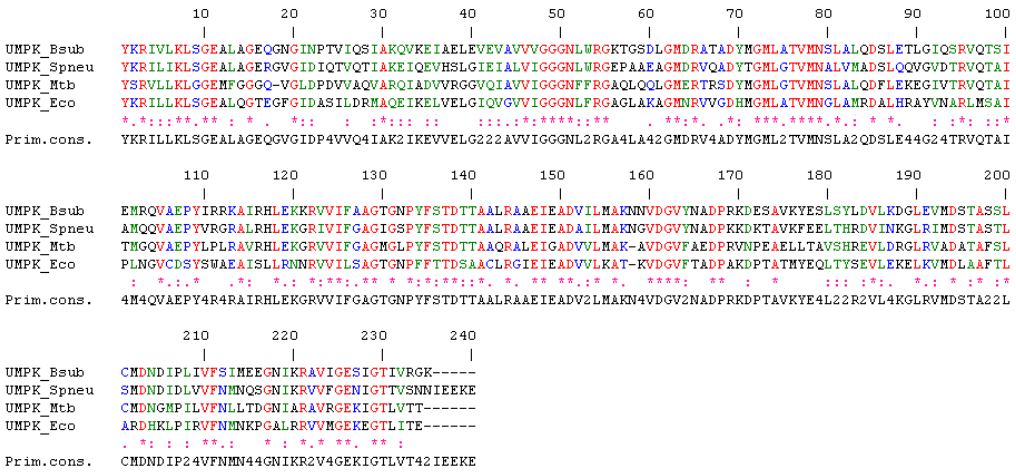

Figura 6. Alinhamento múltiplo das sequências de aminoácidos da proteína *Mt*UMPK (UMPK_Mtb), *B. subtilis* (UMPK_Bsub), *S. pneumoniae* (UMPK_Spneu) e *E. coli* (UMPK_Eco). *, :, · indicam, respectivamente, identidade, similaridade forte e similaridade fraca entre os resíduos de aminoácidos.

A maioria das UMPKs bacterianas, assim como a de *E. coli* (**Figura 7**), possui estrutura homohexamérica, organizada como um trímero de dímeros [31,36,38,40]; e são reguladas pela ativação alostérica de guanosina 5´-trifosfato (GTP) e inibidas por UTP, o que contribui para o equilíbrio da síntese entre nucleosídeos trifosfatados púricos e pirimidínicos (**Figura 8**) [31,36,40].

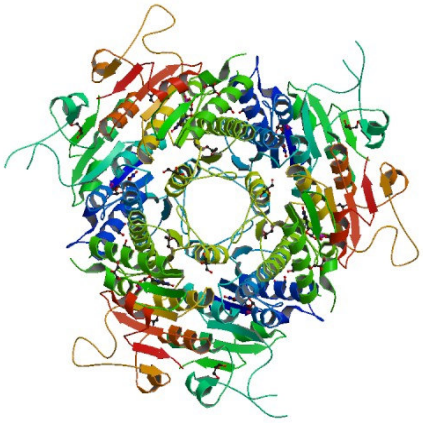

Figura 7. Estrutura da UMPK de *E. coli* (código PDB: 2BNE) em complexo com UMP. Adaptado de Briozzo et al., 2005.

Análises bioquímicas em UMPK de *S. pneumoniae* mostram que o UTP age como um inibidor alostérico, e que não se liga ao sítio ativo da enzima, uma vez que esta não é completamente inibida [40].

No entanto, em estudos com a estrutura cristalográfica da enzima de *E. coli,* resolvida por cristalografia de difração de raios X, a molécula de UTP foi encontrada no sítio aceptor de fosfato, sugerindo que esta seja uma inibição de natureza competitiva, corroborando observações já realizadas de que um excesso de UMP é capaz de reverter o efeito inibidor causado por UTP [31,49].

As enzimas de *E. coli* e *S. pneumoniae* necessitam obrigatoriamente do íon Mg^{2+} como cofator, o qual acredita-se estabilizar o estado de transição durante a transferência do grupo fosfato do ATP para a molécula de UMP, de acordo com a reação: UMP + Mg^{2+}. ATP ↔ UDP + Mg^{2+}. ADP [31,39,40,49].

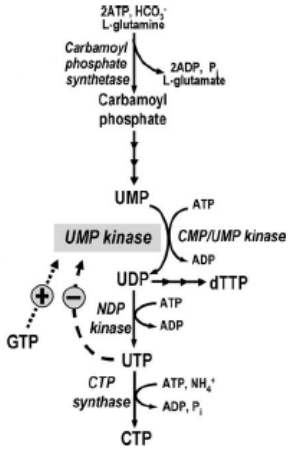

Figura 8. Síntese dos nucleotídeos pirimidínicos e o papel da UMPK em *E. coli*. A UMPK procariótica é destacada em cinza. A CMP/UMP quinase de eucariotos está incluída no esquema. A regulação da enzima por GTP e UTP também pode ser observada. Adaptado de Marco-Marín et al., 2005.

4. OBJETIVOS

4.1 Objetivo geral

Este projeto tem por objetivo a caracterização de um alvo para compostos contra o microrganismo *Mycobacterium tuberculosis* e, portanto, para o tratamento da TB; através da clonagem, expressão, purificação e caracterização bioquímica da provável enzima UMPK de Mtb (EC 2.7.4.-).

4.2 Objetivos específicos

i. Amplificação da região codificante para a *Mt*UMPK através da reação em cadeia da polimerase (PCR);
ii. Clonagem do fragmento amplificado em vetor de clonagem procariótico;
iii. Subclonagem em vetor de expressão pET23a(+);
iv. Expressão da proteína em diferentes cepas de *E. coli* a fim de obtê-la na forma solúvel;
v. Purificação da proteína recombinante através da técnica de FPLC (do inglês, *Fast Protein Liquid Cromatography*);
vi. Quantificação total da proteína;
vii. Verificação da identidade da proteína recombinante purificada, por espectrometria de massas e sequenciamento da região N-terminal da enzima;
viii. Ensaios de atividade enzimática;
ix. Determinação de parâmetros cinéticos através de espectrofotometria;
x. Determinação do mecanismo cinético através da técnica de ITC e das constantes de afinidade de ligação da enzima aos substratos e possíveis inibidores;
xi. Análise de parâmetros termodinâmicos envolvidos na formação do complexo ligante-macromolécula.

5. ARTIGO CIENTÍFICO

TITLE OF THE ARTICLE

UMP kinase from *Mycobacterium tuberculosis*: mode of action and allosteric interactions, and their likely role in pyrimidine metabolism regulation

PERIODIC CHOSEN FOR SUBMISSION

Archives of Biochemistry and Biophysics (impact factor: 2.806).

UMP kinase from *Mycobacterium tuberculosis*: mode of action and allosteric interactions, and their likely role in pyrimidine metabolism regulation[†]

Diana C. Rostirolla[a,b], Ardala Breda[a,b], Leonardo A. Rosado[a,c], Mario S. Palma[d], Luiz A. Basso[a,b*] and Diógenes S. Santos[a,b*]

[a]Centro de Pesquisas em Biologia Molecular e Funcional (CPBMF), Instituto Nacional de Ciência e Tecnologia em Tuberculose (INCT-TB), Pontifícia Universidade Católica do Rio Grande do Sul (PUCRS), 6681/92-A Av. Ipiranga, 90619-900, Porto Alegre, RS, Brazil.

[b]Programa de Pós-Graduação em Biologia Celular e Molecular, Pontifícia Universidade Católica do Rio Grande do Sul (PUCRS), Porto Alegre, RS, Brazil.

[c]Programa de Pós-Graduação em Medicina e Ciências da Saúde, PUCRS, Av. Ipiranga 6681, Porto Alegre, RS 90619-900, Brazil.

[d]Laboratório de Biologia Estrutural e Zooquímica, Centro de Estudos de Insetos Sociais, Departamento de Biologia, Instituto de Biociências de Rio Claro, Universidade Estadual Paulista (UNESP), Rio Claro, SP, Brazil.

[†]This work was supported by the National Institute of Science and Technology on Tuberculosis (DECIT/SCTIE/MS-MCT-CNPq-FNDCT-CAPES) and the Millennium Initiative Program (CNPq) to D.S.S. and L.A.B. D.S.S. (CNPq, 304051/1975-06), L.A.B. (CNPq, 520182/99-5), and M.S.P. (CNPq, 500079/90-0) are Research Career Awardees of the National Research Council of Brazil (CNPq). A.B. is recipient of a PhD student scholarship awarded by BNDES. L.A.R. and D.C.R. are recipients of MSc student scholarships awarded by, respectively, CAPES and CNPq.

Running title: Allosteric interactions of UMP kinase from *Mycobacterium tuberculosis*

*Corresponding authors: Luiz A. Basso or Diógenes S. Santos

Av. Ipiranga 6681 – Tecnopuc – Prédio 92A, ZIP CODE 90619-900, Porto Alegre, RS, Brazil. Phone/Fax: +55 51 33203629; E-mail addresses: luiz.basso@pucrs.br or diogenes@pucrs.br

Abstract

The *pyrH*–encoded uridine 5´-monophosphate kinase (UMPK) is involved in both *de novo* and salvage synthesis of DNA and RNA precursors. Here we describe *Mycobacterium tuberculosis* UMPK (*Mt*UMPK) cloning and expression in *Escherichia coli*. N-terminal amino acid sequencing and electrospray ionization mass spectrometry analyses confirmed the identity of homogeneous *Mt*UMPK. *Mt*UMPK catalyzed the phosphorylation of UMP to UDP, using ATP-Mg^{2+} as phosphate donor. Size exclusion chromatography showed that the protein is a homotetramer. Kinetic studies revealed that *Mt*UMPK exhibits cooperative kinetics towards ATP and undergoes allosteric regulation. GTP and UTP are, respectively, positive and negative effectors, maintaining the balance of purine *versus* pyrimidine synthesis. Initial velocity studies and substrate(s) binding measured by isothermal titration calorimetry suggested that catalysis proceeds by a sequential ordered mechanism, in which ATP binds first followed by UMP binding, and release of products is random. As *Mt*UMPK does not resemble its eukaryotic counterparts, specific inhibitors could be designed to be tested as antitubercular agents.

Keywords: UMPK; cooperative kinetics; allosteric regulation; pyrimidine metabolism; thermodynamic binding parameters; antitubercular drug target.

1. Introduction[1]

Human tuberculosis (TB), mainly caused by *Mycobacterium tuberculosis*, is a major cause of illness and death worldwide. *M. tuberculosis* is a remarkably successful pathogen that latently infects one third of the world population [1] and, despite the availability of effective chemotherapy and moderately protective vaccine, the tubercle bacillus continues to claim more lives than any other single infectious agent [2]. Increasing HIV-TB co-infections [2], the emergence of multidrug-resistant (MDR), extensively drug-resistant (XDR) [3], and, more recently, of totally drug-resistant strains (TDR) [4] have highlighted the need for the development of new therapeutic strategies to combat TB. Strategies based on the discovery of new targets for antimycobacterial agent development include elucidation of the role played by proteins of essential and, preferentially, exclusive biochemical pathways for mycobacterial growth [5].

Rational inhibitor design relies on mechanistic and structural information on the target enzyme. Enzyme inhibitors make up roughly 25 % of the drugs marketed in United States [6]. Enzymes offer unique opportunities for drug design that are not available to cell surface receptors, nuclear hormone receptors, ion channel, transporters, and DNA [6]. It has been pointed out that one of the lessons to be learned from marketed enzyme inhibitors is that the most potent and effective inhibitors take advantage of enzyme chemistry to achieve inhibition

---

[1] *Abbreviations used:* ADP, adenosine 5'-diphosphate; ATP, adenosine 5'-triphosphate; CMP, cytosine 5'-monophosphate; CTP, cytosine 5'-triphosphate; dCMP, deoxycytosine 5'-monophosphate; DMSO, dimethyl sulfoxide; DNA, deoxyribonucleic acid; dTMP, deoxythymidine 5'-monophosphate; ESI-MS, electrospray ionization mass spectrometry; FDA, Food and Drug Administration; GTP, guanosine 5'-triphosphate; HEPES, *N*-2-hydroxyethylpiperazyne-*N'*-2-ethanesulfonic acid; HIV, human immunodeficiency virus; IPTG, isopropyl-β-D-thiogalactopyranoside; ITC, isothermal titration calorimetry; LB, Luria-Bertani; MDR, multidrug-resistant; *Mt*UMPK, uridine 5'-monophosphate kinase from *Mycobacterium tuberculosis*; NADH, nicotinamide adenine dinucleotide; NDP, nucleoside diphosphate; NMP, nucleoside monophosphate; NTP, nucleoside triphosphate; PCR, polymerase chain reaction; PDB, Protein Data Bank; RNA, ribonucleic acid; SDS-PAGE, sodium dodecyl sulfate-polyacrylamide gel eletrophoresis; TB, Terrific Broth; TB, tuberculosis; Tris, tris(hydroxymethyl)aminomethane; UDP, uridine 5'-diphosphate; UMP, uridine 5'-monophosphate; UMPK, uridine 5'-monophosphate kinase; UTP, uridine 5'-triphosphate; XDR, extensively drug-resistant.

[7]. Moreover, the recognition of the limitations of high-throughput screening approaches in the discovery of candidate drugs has rekindled interest in rational design methods [8]. Accordingly, mechanistic analysis should always be a top priority for enzyme-targeted drug programs aiming at the rational design of potent enzyme inhibitors.

Nucleotides are important molecules present in all living organisms as they constitute the building blocks for nucleic acids and also serve as energy sources for many biochemical reactions [9]. Pyrimidine nucleotides can be synthesized by *de novo* and salvage pathways resulting in a common product, the nucleotide uridine 5´-monophosphate (UMP) [10]. Subsequent phosphorylation of UMP yields UDP that leads to the synthesis of all other pyrimidine nucleotides [11]. Nucleoside monophosphate (NMP) kinases play an important role in the biosynthesis of nucleotides and represent a homogeneous family of catalysts related to adenylate kinase (EC 2.7.4.3). They catalyze the synthesis of nucleoside diphosphates (NDPs), which will be converted to nucleoside triphosphates (NTPs) by a non-specific nucleoside diphosphate kinase [12]. UMP kinases (UMPKs) catalyze the reversible transfer of the γ-phosphoryl group from ATP to UMP in the presence of a divalent cation, usually Mg^{2+} (**Fig. 1**) [13]. In general, eukaryotic UMP/CMP kinases (EC 2.7.4.14) are monomers, phosphorylate with comparable efficiency both UMP and CMP, and are structurally similar to other NMP kinases (such as adenylate kinase) [12,14-16]. In contrast, bacterial UMPKs (EC 2.7.4.22) are specific for UMP, exist in solution as stable homohexamers, and do not resemble either UMP/CMP kinases or NMP kinases from other organisms based on sequence comparisons [17,18]. Kinetic studies have shown that bacterial UMPKs can be activated by GTP and/or be subject to feedback inhibition by UTP, the major product of the reaction they catalyze [17-21], regulating the balance of purine *versus* pyrimidine nucleoside triphosphates synthesis [13].

As pyrimidine biosynthesis is an essential step in the progression of TB, enzymes of this pathway are attractive antitubercular drug targets [22]. Homologues to enzymes in the pyrimidine pathway have been identified in the genome sequence of *M. tuberculosis* [23]. A rapid recombination method for screening and confirmation of gene essentiality has recently been proposed to allow identification of which of the approximately 4,000 genes of *M. tuberculosis* are worthy of further study as drug targets [24]. The product of *pyrH* (Rv2883) gene has been shown to be essential for *M. tuberculosis* growth by the rapid screening method [24]. Genetic studies have provided evidence that UMPK is essential for growth in both Gram-negative (*Escherichia coli*) [25,26] and Gram-positive bacteria (*Streptococcus pneumoniae*) [19]. Although the *pyrH* gene has been proposed by sequence homology to encode a UMPK protein [23], there has been no formal biochemical proof as to ascertain the correct assignment to the open reading frame of *pyrH* gene in *M. tuberculosis*.

In the present work, the *pyrH* gene from *M. tuberculosis* strain H37Rv was PCR amplified, cloned, and recombinant UMPK (*Mt*UMPK) was purified to homogeneity. N-terminal amino acid sequencing and electrospray ionization mass spectrometry (ESI-MS) analyses were carried out to confirm the identity of the recombinant *Mt*UMPK protein. Initial velocity studies were performed to evaluate the kinetic parameters of the recombinant *Mt*UMPK. In addition, isothermal titration calorimetry study of substrates binding was carried out to demonstrate the order of substrate addition in the kinetic mechanism of *Mt*UMPK. Protein allosteric regulation by ATP, GTP and UTP have also been demonstrated. These results represent an important step for the rational design of *Mt*UMPK inhibitors that can further be tested as anti-TB drugs.

2. Materials and methods

2.1 Amplification, cloning and DNA sequencing of the pyrH gene

The full-length *pyrH* (Rv2883c) coding region [23] was PCR amplified using the genomic DNA from *M. tuberculosis* H37Rv as template and a high fidelity proof-reading thermostable DNA polymerase (*Pfu*® DNA polymerase, Stratagene). The synthetic oligonucleotides used (forward primer, 5′-GTC ATA TGA CAG AGC CCG ATG TCG CCG GC-3′; and reverse primer, 5′-TAA AGC TTT CAG GTG GTG ACC AGC GTT CCG A-3′) were designed to contain, respectively, *Nde*I and *Hind*III (New England Biolabs) restriction sites (underlined). Dimethyl sulfoxide (DMSO) was added to a final concentration of 10%. The 786-bp amplicon was detected on 1% agarose gel and purified utilizing the Quick Gel Extraction kit (Invitrogen). The PCR fragment was cloned into pCR-Blunt® vector (Invitrogen) and, following transformation of *E. coli* strain DH10B (Novagen), the resulting plasmid was isolated utilizing the Qiaprep Spin Miniprep kit (Qiagen). Subsequently, the fragment was cleaved with *Nde*I and *Hind*III endonucleases and inserted into the pET-23a(+) expression vector (Novagen), previously digested with the same restriction enzymes. The complete *pyrH* nucleotide sequence was determined by automated DNA sequencing to corroborate sequence identity, integrity and to check the absence of mutations in the cloned fragment.

2.2 Expression and purification of recombinant MtUMPK

The recombinant plasmid pET-23a(+)::*pyrH* was transformed into BL21(DE3) *E. coli* electrocompetent cells (Novagen), and cells carrying the recombinant vector were selected on Luria-Bertani (LB) agar plates containing 50 μg mL^{-1} ampicillin [27]. A single colony was used to inoculate 50 mL of Terrific Broth (TB) medium containing the same antibiotic and

grown overnight at 37 ºC. Aliquots of this culture (2.5 mL) were used to inoculate 250 mL of TB medium in 5 x 1 L flasks supplemented with ampicillin (50 µg mL^{-1}) and grown at 37 ºC and 180 rpm to an optical density (OD_{600nm}) of 0.4 – 0.6. When this OD_{600} value was reached, the temperature was lowered to 30 ºC and protein expression was carried out without isopropyl-β-D-thiogalactopyranoside (IPTG) induction. After 24 h, the cells (12 g) were collected by centrifugation at 11,800*g* for 30 min at 4°C and stored at -20 ºC. The same protocol was employed for BL21 (DE3) *E. coli* cell transformed with pET-23a(+) as control. The expression of the recombinant protein was confirmed by 12 % sodium dodecyl sulfate-polyacrylamide gel eletrophoresis (SDS-PAGE) stained with Coomassie Brilliant Blue [28].

E. coli (2 g) cells overproducing the *Mt*UMPK were resuspended in 20 mL of 50 mM Tris HCl pH 7.5 (buffer A), stirred for 30 min at 4 ºC in the presence of lisozyme (0.2 mg mL^{-1}, Sigma-Aldrich), and disrupted by sonication (eight pulses of 10 s, at an amplitude value of 60%). The lysate was centrifuged at 38,900*g* for 30 min to remove cell debris and the supernatant was treated with 1% (wt/vol) streptomycin sulfate (Sigma-Aldrich), stirred for 30 min, and the mixture was centrifuged at 38,900*g* for 30 min. The supernatant containing soluble *Mt*UMPK was dialyzed against 2 L of buffer A for 3 hours.

All purification steps were carried out on an ÄKTA system (GE Healthcare) at 4 ºC with UV detection at 215, 254 and 280 nm, and fractions were analyzed by SDS-PAGE. The crude extract was loaded on a HiPrep 16/10 Q XL (GE Healthcare) anion exchange column pre-equilibrated with buffer A. Proteins were eluted using a 0–300 mM NaCl linear gradient at a flow rate of 1 mL min^{-1}. Fractions containing *Mt*UMPK in NaCl (*ca.* 280 mM) were pooled and $(NH_4)_2SO_4$ was added to a final concentration of 1 M, stirred for 30 min, and clarified by centrifugation at 38,900*g* for 30 min. The supernatant was loaded on a Butyl Sepharose High Performance (GE Healthcare) hydrophobic interaction column pre-equilibrated with 50 mM Tris HCl pH 7.5 containing 1 M $(NH_4)_2SO_4$. Proteins were eluted

using a 0–100 % linear gradient of buffer A at a flow rate of 1 mL min^{-1}. Pooled fractions containing *Mt*UMPK was dialyzed against buffer A to remove salt and loaded on a Mono Q 16/10 (GE Healthcare) anion exchange column. *Mt*UMPK was eluted in a salt gradient (0–240 mM NaCl) at a flow rate of 1 mL min^{-1}. The pooled sample was dialyzed against 50 mM Tris HCl pH 7.5 containing 200 mM NaCl, concentrated using an AMICON (Millipore Corporation, Bedford, MA) ultra filtration membrane (MWCO = 10 kDa), and stored at -80 ºC. Total protein concentration was determined by the method of Bradford [29], using the Bio-Rad protein assay kit (Bio-Rad Laboratories) and bovine serum albumin as standard.

2.3 Amino acid sequence and mass spectrometry analysis

The N-terminal amino acid residues of homogenous recombinant *Mt*UMPK were determined by automated Edman degradation sequencing using a PPSQ-21A gas-phase sequencer (Shimadzu) [30]. Recombinant *Mt*UMPK was analyzed by electrospray ionization mass spectrometry (ESI-MS) employing some adaptations made to the system described by Chassaigne and Lobinski [31]. Samples were analyzed on a Quattro-II triple-quadrupole mass spectrometer (Micromass; Altrincham, UK), using MassLynx and Transform softwares for data acquisition and spectrum handling.

2.4 Determination of MtUMPK molecular mass

Gel filtration chromatography was performed on a Superdex 200 (HR 10/30) column (GE Healthcare) pre-equilibrated with 50 mM Tris HCl pH 7.5 containing 200 mM NaCl at a flow rate of 0.4 mL min^{-1}, with UV detection at 215, 254 and 280 nm. The LMW and HMW Gel Filtration Calibration Kits (GE Healthcare) were used to prepare a calibration curve. The

elution volumes (V_e) of standard proteins (ferritin, catalase, aldolase, coalbumin, ovalbumin, ribonuclease A) were used to calculate their corresponding partition coefficient (K_{av}, Eq. 1). Blue dextran 2000 (GE Healthcare) was used to determine the void volume (V_o). V_t is the total bead volume of the column. The K_{av} value for each protein was plotted against their corresponding molecular mass.

$$K_{av} = \frac{V_e - V_o}{V_t - V_o} \qquad \text{Eq. 1}$$

2.5 Multiple sequence alignment

The amino acid sequences of the following UMPK proteins, whose three-dimensional structures were solved, were included in the alignment: *E. coli* (NP_414713.1)*, Ureaplasma parvum* (YP_001752598.1), *Pyrococcus furiosus* (NP_579136.1), *Sulfolobus solfataricus* (NP_342460.1), and *Bacillus anthracis* (NC_012659.1). The UMPK amino acid sequences of *S. pneumoniae* (YP_816317.1) and *Bacillus subtilis* (NP_389533.2) [32] were also included in the alignment and compared with *M. tuberculosis* UMPK (NP_217399.1). Multiple amino acid sequence alignment was performed by ClustalW [33], using the Gonnet matrix for amino acids substitutions and considering gap penalties, to identify essential residues for nucleotide substrate(s) binding, as well as to infer possible similarities in their mechanism of catalysis. For alignment improvement, 8, 23, 11, 5, 5 and 29 amino acids residues were removed from the *E. coli*, *U. parvum*, *B. anthracis*, *S. pneumoniae*, *B. subtilis* and *M. tuberculosis*, respectively.

2.6 Functional characterization of MtUMPK

*Mt*UMPK catalytic activity was measured for all purification steps in the forward direction at 25 ºC, using a coupled spectrophotometric assay (0.5 mL final volume) as described elsewhere [34], on an UV-2550 UV/Visible spectrophotometer (Shimadzu). In short, the reaction mixture contained 50 mM Tris HCl pH 7.5, 50 mM KCl, 5 mM $MgCl_2$ buffer; 1 mM phosphoenolpyruvate, 0.2 mM ß-NADH, fixed concentrations of both ATP (3000 μM) and UMP (600 μM) substrates, 3 units of pyruvate kinase (EC 2.7.1.40) and 2.5 units of L-lactate dehydrogenase (EC 1.1.1.27). The reaction was started by the addition of *Mt*UMPK. The decrease in absorbance at 340 nm ($\varepsilon_{\beta\text{-NADH}} = 6.22 \times 10^{-3}\ M^{-1}.cm^{-1}$) was continuously monitored and corrected for non-catalyzed chemical reactions in the absence of UMP. One unit of *Mt*UMPK is defined as the amount of enzyme necessary to convert 1 μmol of UMP in UDP per min in an optical path of 1 cm.

2.7 Steady-state kinetics

Determination of the apparent steady-state kinetic parameters were evaluated at varying concentrations of UMP (0–150 μM) and a fixed-saturating concentration of ATP (3000 μM), and at varying concentrations of ATP (0–3000 μM) and a fixed-saturating level of UMP (600 μM). Initial velocity data were analyzed by SigmaPlot (Systat Software, Inc.).

In order to evaluate the specificity for phosphate acceptor, UMP was replaced with other nucleoside monophosphates (CMP, dCMP or dTMP) at different concentrations. The specificity of the enzyme as regards the phosphoryl donors was tested by replacing ATP with 3 mM GTP, CTP and UTP in the standard assay.

Inhibition studies were carried out in the presence of fixed non-saturating levels of ATP (1300 μM) and fixed-varied UTP concentration (0, 30, 50, and 70 μM) when UMP was

the variable substrate. Inhibition studies were also carried out in the presence of fixed non-saturating concentration of UMP (40 μM) and fixed-varied UTP concentration (0, 20, 50, and 100 μM) when ATP was the variable substrate. In addition, saturation curves for UTP (0 μM–400 μM) were carried out at three different sets of experiments: fixed-non-saturating ATP concentration (1300 μM) corresponding to its $K_{0.5}$, and saturating UMP concentration (600 μM = 19 x K_m); fixed-non-saturating ATP concentration (1300 μM) corresponding to its $K_{0.5}$, and non-saturating UMP concentration (30 μM ≅ K_m); and fixed saturating ATP concentration (3000 μM = 2.3 x $K_{0.5}$) and non-saturating UMP concentration (30 μM ≅ K_m). The maximal rate for each reaction condition was determined in the absence of inhibitor. Initial velocity parameters were also analyzed as a function of ATP concentrations at fixed-saturating UMP concentration (600 μM) either in the absence or presence of a fixed concentration of GTP (500 μM) to verify whether this substrate has any effect on the kinetic properties of *Mt*UMPK (70 nM). Initial velocity measurements were also carried out as a function of UMP concentration at fixed-saturating ATP concentration (3000 μM) in either absence or presence of GTP (500 μM).

Hyperbolic saturation curves were fitted by nonlinear regression analysis to the Michaelis-Menten equation (Eq. 2), in which v is the steady-state velocity, V_{max} is the maximal rate, [S] is the substrate concentration, and K_m is the Michaelis-Menten constant [35,36]. Sigmoidal curves were fitted to the Hill equation (Eq. 3), where $K_{0.5}$ is the value of the substrate concentration where $v = 0.5\ V_{max}$, and n is the Hill coefficient (indicating the cooperative index) [35,36].

$$v = \frac{V_{max}[S]}{K_m + [S]} \qquad \text{Eq. 2}$$

$$v = \frac{V_{\max}[S]^n}{K_{0.5}^n + [S]^n} \qquad \text{Eq. 3}$$

The K_i value for UTP towards UMP was calculated using the uncompetitive equation (Eq. 4), in which [I] is the inhibitor concentration and K_i is the inhibition constant [35,36].

$$v = \frac{V_{\max}[S]}{[S]\left(1 + \frac{[I]}{K_i}\right) + K_m} \qquad \text{Eq. 4}$$

The IC_{50} value, which defines the concentration of inhibitor required to half-saturate the enzyme population, was determined by fitting the data to Eq. 5, in which v_i and v_o are, respectively, the reaction velocity in the presence and in the absence of inhibitor, v_i/v_o represents the fractional activity remaining at a given inhibitor concentration (fraction of free enzyme), and n is the Hill coefficient [36].

$$\frac{v_i}{v_o} = \frac{1}{1 + \left(\frac{[I]}{IC_{50}}\right)^n} \qquad \text{Eq. 5}$$

2.8 Isothermal Titration Calorimetry (ITC)

ITC experiments were carried out using an iTC_{200} Microcalorimeter (MicroCal, Inc., Northampton, MA). The reference cell (200 µL) was loaded with Milli Q water during all experiments and the sample cell (200 µL) was filled with *Mt*UMPK at a concentration of 100 µM. The injection syringe (39.7 µL) contained substrates or effectors at different concentrations: ATP, ADP, GTP, and UTP at 1.5 mM, UMP at 3 mM, and UDP at 1.8 mM.

The ligand binding isotherms were measured by direct titration (ligand into macromolecule). The enzyme was prepared for ITC analysis by dialysis against 50 mM HEPES at pH 7.5 containing 50 mM KCl, 5 mM $MgCl_2$, 200 mM NaCl. The same buffer was used to prepare all ligand solutions and Tris, used at the kinetic assays, was replaced with HEPES due to the high enthalpy of ionization of Tris [37,38]. The stirring speed was 500 rpm at a temperature of 25 ºC for all ITC experiments. The first titration injection (0.5 µL), which was discarded in the data analysis, was followed by 17 injections of 2.2 µL each at 180 s intervals. Control titrations (ligand into buffer) were performed to subtract the heats of dilution and mixing for each experiment prior to data analysis. The data after peak integration of the isotherm generated by ITC, subtraction of control titration data and concentration normalization (heat normalized to the molar ratio), were analyzed by Origin 7 SR4 software (Microcal, Inc.).

The ΔG (Gibbs free energy) of binding was calculated using the relationship described in Eq. 6, in which R is the gas constant (8.314 J K^{-1} mol^{-1}), T is the temperature in Kelvin (T = °C + 273.15), and K_a is the association constant at equilibrium. The entropy of binding (ΔS) can also be determined by this mathematical formula. The initial estimates for n, K_a, and ΔH parameters were refined by standard Marquardt nonlinear regression method provided in the Origin 7 SR4 software.

$$\Delta G^o = -RT \ln K_a = \Delta H^o - T\Delta S^o \qquad \text{Eq. 6}$$

3. Results and discussion

3.1 Amplification, cloning and sequencing of the pyrH gene

The 786-bp PCR amplicon was consistent with the *M. tuberculosis* H37Rv *pyrH* coding region (data not shown). The product was purified and ligated into pET-23a(+) expression vector as described in section 2.1. Automated DNA sequencing confirmed the identity and the absence of mutations in the cloned fragment.

3.2 Expression and purification of the recombinant MtUMPK

The resulting pET-23a(+)::*pyrH* recombinant plasmid was electroporated into BL21(DE3) *E. coli* cells and cultures were grown in TB medium for 24 hours. Analysis by SDS-PAGE indicated that the supernatant of cell extract (**Fig. 2A, lane 3**), which was sonicated and centrifuged, contained a significant amount of protein with subunit molecular mass (*ca*. 27 kDa) in agreement with the predicted MW for *Mt*UMPK (27.4 kDa).

The overexpressed protein was purified by a three-step protocol consisting of an anion-exchange column (HiPrep Q XL), a hydrophobic interaction column (Butyl Sepharose HP) and a strong anion-exchange column (Mono Q). The target protein eluted at approximately 180 mM of NaCl from the Mono Q column, and SDS-PAGE analysis showed that recombinant *Mt*UMPK was homogenous (**Fig. 2B, lane 5**). This 1.7-fold purification protocol yielded 20 mg of recombinant protein from 2 g of cells, indicating a 21 % protein yield (**Table 1**). Enzyme kinetic measurements by NADH-coupled spectrophotometric assay showed that recombinant *Mt*UMPK indeed catalyzes the phosphorylation of UMP. Nevertheless, increase in the specific activity could be observed in the presence of high salt concentrations and a pronounced decrease after salt removal. This difference in activity may be attributed to ionic strength which, such as pH variations, is recognized to affect enzyme conformation, stability and activity [39,40]. Gagyi et al. [18] have also reported the addition of 100 mM NaCl as an approach to keep the *B. subtilis* UMPK stability. Accordingly, the

homogenous protein was stored at -80 ºC 50 mM Tris HCl pH 7.5 buffer containing 200 mM NaCl, which resulted in an apparent maximum velocity of 7.67 U mg^{-1} and allowed the kinetic assays to be carried out without affecting the coupled enzymes.

3.3 Mass spectrometry and N-terminal amino acid sequencing

The subunit molecular mass value was determined to be 27 264.08 ± 13 Da by ESI-MS, which is lower than expected from the predicted amino acid sequence (27 395.00 Da), indicating that the N-terminal methionine (130.92 Da) was removed.

The first 22 N-terminal amino acid residues identified by the Edman degradation method correspond to those predicted for the *pyrH* gene protein product and corroborate the N-terminal methionine removal. These results unambiguously identify the homogenous recombinant protein as the putative *Mt*UMPK.

3.4 MtUMPK molecular mass determination

The molecular mass of the native enzyme was determined by gel-filtration chromatography and yielded a single peak with elution volume corresponding to approximately 106 kDa, suggesting that *Mt*UMPK is a tetramer in solution (106,000 Da/27 264.08 Da ≅ 3.9), differing from other bacterial homohexameric UMPKs [17-19].

3.5 Multiple sequence alignment

The currently available three-dimensional structures of UMPKs from several prokaryotic organisms deposited in the Protein Data Bank, such as *E. coli* (PDB code: 2BNE,

2BND, 2BNF and 2V4Y) [13,41] , *U. parvum* (PDB code: 2VA1) [21], *P. furiosus* (PDB code: 2BRI and 2BMU) [11], *S. solfataricus* (PDB code: 2J4J, 2J4K and 2J4L) [20] and *B. anthracis* (PDB code: 2JJX) [9], allow drug design based on a detailed model of the target binding site. The experimentally solved structures of *E. coli* UMPK [13,41] in complex with its substrates and the allosteric effector permit to propose the amino acid side chains in *M. tuberculosis* that are involved in ATP, UMP, and UDP binding as well as residues that participate in GTP binding. To this end, multiple sequence alignment was carried out and the results suggest that the conserved *Mt*UMPK Gly83 and Asp97 (*M. tuberculosis* numbering) amino acid residues are equivalent to residues in *E. coli* UMPK [13] that interact with the 2′-OH ribose ring of UMP (**Fig. 3**). The amino acids Gly77, Gly78, Arg82 and Thr165, which are involved in UMP α-phosphate interactions, are conserved among all sequences aligned. The main differences among UMP binding residues are those associated with uracil binding. The interactions between *E. coli* UMPK and the uracil moiety of UMP are between the hydrophilic Thr138 and Asn140 amino acids, whereas in *Mt*UMPK these interactions are made by the hydrophobic Met158 and Leu160 residues. As no structural data for *Mt*UMPK have been available to date, it is tempting to suggest that these differences may be related to the distinct quaternary structures of *Mt*UMPK (tetramer) and *E. coli* UMPK (hexamer), since site-directed mutagenesis of Thr138 and Asn140 residues suggested their involvement in subunit contacts in the quaternary structure of the latter [13]. The interactions between the enzyme and uracil, ribose, or the UDP α-phosphate moiety are very similar to those with UMP, although UDP binding involves three additional amino acid residues [13]. The Lys36 and Gly39 residues (*M. tuberculosis* numbering) are conserved, whereas Gly39 in *Mt*UMPK sequence replaces a serine residue present in *E. coli* UMPK.

The amino acids Lys36, Asp166, Phe191, Asp194 and Asp221 in *Mt*UMPK are likely involved in ATP interaction since they are conserved in the *E. coli* UMPK and *Mt*UMPK

polypeptide sequences. On the other hand, Lys185 in *Mt*UMPK replaces a threonine residue present in ATP binding site of *E. coli* UMPK. It is interesting to note that the Lys residue involved in ATP binding replaces Thr in five UMPK sequences [43] as in *Mt*UMPK. In *E. coli* UMPK, the GTP-binding site is between two dimers of the hexamer and GTP promotes a rearrangement of its quaternary structure, resulting in a tighter dimer-dimer interaction [41]. Asp113, which interacts with the GTP purine moiety, Arg123 and Arg150, both interacting with the phosphate group, are the most conserved amino acid residues (**Fig. 3**). These residues are absent in *U. parvum* and *S. solfataricus* UMPKs and may explain the lack of GTP stimulation of these enzymes [20,21].

3.6 MtUMPK kinetic parameters

The dependence of velocity with UMP as variable substrate at fixed-saturating ATP concentration (3000 μM) followed hyperbolic Michaelis-Menten kinetics (**Fig. 4A**), and the apparent constant values were thus calculated fitting the data to Eq. 2, yielding the following values: V_{max} = 7.5 (± 0.3) U mg^{-1} and K_m = 31 (± 3) μM. These results permit estimate a value of 3.4 (± 0.1) s^{-1} for the UMP catalytic constant (k_{cat}) and of 11 (± 1) x 10^4 $M^{-1}s^{-1}$ for the UMP specificity constant (k_{cat}/K_m). The Michaelis-Menten constant values are similar to those reported for *B. subtilis* (K_m^{UMP} = 30 μM) and *E. coli* (K_m^{UMP} = 43 μM at pH 7.4) UMPKs [18,41].

The saturation curve for ATP at fixed-saturating UMP concentration (600 μM) was sigmoidal (**Fig. 4B**), suggesting cooperative kinetics. Accordingly, the data were fitted to the Hill equation (Eq. 3), yielding the following values: V_{max} = 8.8 (± 0.2) U mg^{-1}, $K_{0.5}$ = 1299 (± 32) μM and n = 3.9 (± 0.3). The k_{cat} for ATP is 4.0 (± 0.1) s^{-1}. The limiting value for the Hill

coefficient (*n*) is four since we showed that *Mt*UMPK is a homotetramer in solution. The *n* value of 3.9 thus indicates strong positive cooperativity for ATP.

As demonstrated for others UMPKs [17,20,21], *Mt*UMPK was specific for UMP as the phosphoryl group acceptor as no enzyme activity was detected with CMP, dCMP or dTMP. The specificity for the phosphoryl group donor was tested with GTP, CTP and UTP, and UMP as the acceptor substrate. No activity was detected with GTP and CTP. UTP acted as phosphoryl donor at a velocity value of 0.5 U mg^{-1}. This value is 18-fold lower than for ATP (8.8 U mg^{-1}), suggesting that ATP is the more likely physiological phosphate donor for *Mt*UMPK.

UTP has been reported as a common negative regulator of UMPKs from Gram-negative bacteria, Gram-positive bacteria and archae [20,42,43]. To evaluate the inhibitory effect of UTP on *Mt*UMPK enzyme velocity, measurements of steady-state rates were carried out as described in the Materials and methods section. Double-reciprocal plots at different UTP concentrations displayed a pattern of parallel lines, suggesting that UTP acts as an uncompetitive inhibitor towards UMP in which V_{max} and K_m values were simultaneously reduced (**Fig. 5**) at fixed non-saturating ATP concentration (1300 μM) and varying UMP concentration. Data fitting to Eq. 4 for uncompetitive inhibition yielded a K_i value of 87 (± 5) μM for UTP. On the other hand, the plots of *Mt*UMPK activity versus ATP concentration in the presence of both non-saturating UMP (40 μM) and fixed-varied UTP concentrations (0, 30, 50, and 70 μM) were all sigmoidal. Although inhibition by UTP did not modify the sigmoidal shape of the curve, data fitting to Eq. 3 yielded increasing, though modest, values for apparent $K_{0.5}$, whereas V_{max} and the Hill coefficient values remained approximately constant (**Table 2**). These features appear to be a common theme for UMPKs from Gram-positive and archae microorganisms [19,20,43].

The saturation curves for UTP inhibition in the presence of fixed-non-saturating ATP concentration and saturating UMP concentration, fixed-non-saturating ATP concentration and non-saturating UMP concentration, and fixed saturating ATP concentration and non-saturating UMP concentration were all sigmoidal (data not shown). These data were thus fitted to Eq. 5, yielding estimates for IC_{50} values and the Hill coefficient (**Table 3**). The rates decreased with increasing UTP concentration, reaching a plateau of low enzyme activity (below 0.5 U mg^{-1}) at high UTP concentrations. The IC_{50} values of 80 μM (saturating UMP concentration) and 97 μM (non-saturating UMP concentration) were within experimental error. These results are in agreement with UTP acting as an uncompetitive inhibitor towards UMP (**Fig. 5**), thereby suggesting that UTP preferentially binds to a complex formed between *Mt*UMPK and UMP (it would have to be a ternary complex because we showed that ATP binding is followed by UMP binding). This type of inhibition cannot be overcome by high UMP substrate concentrations, suggesting that UTP binds to an allosteric (regulatory) site. In addition, there was a decrease in the Hill coefficient (n) from 2.8 at non-saturating UMP concentration to 1.5 at saturating UMP concentration (**Table 3**). It thus appears that increasing UMP concentration results in decreasing degree of cooperativity. In the presence of saturating ATP concentration (3000 μM), there was a 2-fold increase in IC_{50} value for UTP, suggesting that UTP acts as a competitive inhibitor towards ATP. These data are consistent with ATP kinetics in which increasing fixed-varied concentrations of UTP in the presence of fixed-non-saturating UMP concentration yielded increasing values for apparent $K_{0.5}$ (Table 2). Moreover, since we have shown that UTP can act as a poor phosphoryl donor, it is thus likely that UTP can also bind to ATP binding site of *Mt*UMPK. These data suggest that UTP either binds to the ATP binding site with low affinity or to an allosteric site that results in uncompetitive inhibition towards UMP. Incidentally, it has been proposed that each subunit of bacterial UMPKs has three distinct nucleotide-binding sites [43].

GTP has been shown to be a positive effector for bacterial UMPKs [41,43]. The crystal structure of *E. coli* UMPK bound to GTP has recently been solved at 2.3 Å [41]. The presence of GTP (500 μM) resulted in both increased V_{max} values (from 2 to 3.2 U mg^{-1}) and affinity ($K_{0.5}$) of ATP for *Mt*UMPK (from 1335 to 545 μM) (**Fig. 6**). In addition, the Hill coefficient value of 4.4 in the absence of GTP decreased to 1.6 in the presence of GTP (500 μM), suggesting that this nucleotide decreased the degree of cooperativity of ATP upon *Mt*UMPK enzyme activity (**Fig. 6**). These results are in agreement with previously published results on UMPKs from Gram-positive bacteria [19,43]. On the other hand, the effect of GTP on UMP kinetics displayed a slight increase in the V_{max} values (from 1.63 ± 0.03 U mg^{-1} in the absence to 2.07 ± 0.05 U mg^{-1} in the presence of GTP), and no change of K_m values for UMP (data not shown).

3.7 Equilibrium binding of ligands assessed by ITC

To further elucidate the *Mt*UMPK kinetic mechanism, titration microcalorimetry of ligand binding to the recombinant enzyme was carried out. Equilibrium binding values of ligands were measured directly by ITC, determining the heat generated or consumed upon ligand-macromolecule binary complex formation at constant temperature and pressure. The measured of the heat released upon binding of the ligands allowed us to derive the binding enthalpy (ΔH) of the process, to estimate the stoichiometry of the interaction (n) and the association constant at equilibrium (K_a). The dissociation constant at equilibrium (K_d) could be calculated as the inverse of K_a ($K_d = 1/K_a$). Moreover, the Gibbs free energy (ΔG) and entropy (ΔS) of binding were determined from the association constant values at equilibrium as described in Eq. 6. The ITC data for binding of ligands to *Mt*UMPK (**Fig. 7**) are summarized in **Table 4**. The overall binding isotherms for ATP, ADP, UDP or GTP binding

to *Mt*UMPK were best fitted to a model of one set of sites (**Table 4**). The UTP binding isotherm was not well defined to obtain an adequate fit of the data to any model, probable because this substrate may exert different and simultaneous effects on *Mt*UMPK.

The mechanism of phosphoryl transfer of NMP kinases has been reported to follow a sequential random bi bi kinetic mechanism [12]. The *Mt*UMPK appears to deviate from this type of mechanism, since no significant heat changes were obtained for UMP binding, suggesting that it cannot bind to free enzyme. In contrast, all other ligands tested do bind to the free enzyme and exhibit exothermic reactions, as seen by negative changes in the binding enthalpy (**Fig. 7**). Interestingly, the binding isotherm of an ATP molecule does not appear to influence the affinity for the subsequent one, as the thermodynamic parameters for ATP binding provide single ΔH and K_a values. How can one reconcile these data with positive cooperativity displayed by the saturation curve (**Fig. 4B**) of steady-state kinetics for ATP in the presence of UMP? These data suggest that ATP binding has a positive heterotropic effect upon UMP binding to *Mt*UMPK:ATP binary complex, since UMP does not bind to the free enzyme. The *n* value of 0.57 sites for the ATP binding refers to the event of two subunits of *Mt*UMPK in the cell associating with each ATP molecule injected. In summary, we propose that ATP binding triggers a conformational change of *Mt*UMPK that results in increased affinity for UMP.

The UDP product binds to free *Mt*UMPK enzyme with higher affinity than ADP product (**Table 4**), and both ligands displayed a stoichiometry of one ligand binding to each monomer of the tetrameric enzyme. The larger association constant of UDP as compared to ADP appears to be enthalpy driven (**Table 4**). These ITC results suggest that product release is random. The GTP binding affinity is in the same range of UDP (**Table 4**). These ITC results demonstrate that GTP is capable of binding to free *Mt*UMPK enzyme with a stoichiometry close to unity. It is interesting to note that ATP (substrate) as compared to ADP

(product) binding display approximately the same association constant at equilibrium (or Gibbs free energy), which is a result of the ubiquitous phenomenon of enthalpy-entropy compensation meaning that entropy losses often negate enthalpy gains [8]. In short, ITC and steady-state kinetic results provide evidence *Mt*UMPK follows an sequential ordered mechanism, in which ATP binds first to free enzyme followed by UMP binding to the *Mt*UMPK:ATP binary complex (**Fig. 8**). Release of products is however random. The mechanism for *S. solfataricus* UMPK has been shown to be random order for either addition of substrates or release of products [20].

4. Summary

Bacterial UMPKs have been proposed to be attractive drug targets because their primary amino acid sequence and three-dimensional structures are divergent from their eukaryotic counterparts. They are unique members of the NMP kinases family of enzymes and several research groups have demonstrate its essentiality for different organisms [17,19,25,26,44], and to *M. tuberculosis* in particular [24]. Moreover, they are oligomers with an exclusive and complex control of activity by GTP and UTP, representing an interesting model of allosteric regulation [43]. The elucidation of the mode of action of *Mt*UMPK is thus warranted. Although the *pyrH* gene has been proposed by *in silico* analysis to encode a UMPK enzyme [23], formal biochemical proof was still lacking as regards the correct assignment to its open reading frame in *M. tuberculosis*. Accordingly, here we describe PCR amplification of the *pyrH* coding region, cloning, heterologous expression, and purification of recombinant protein to homogeneity. N-terminal amino acid sequence and ESI-MS confirmed the identity of the homogeneous recombinant protein. Steady-state kinetic measurements confirmed that the *pyrH* gene encodes a UMPK enzyme in *M. tuberculosis*. Size exclusion

chromatography showed that *Mt*UMPK is a tetramer in solution. Multiple sequence alignment analysis allowed identification of residues involved in substrate binding and/or catalysis.

Steady-state kinetic measurements showed that *Mt*UMPK is specific for both ATP and UMP substrates. This specificity for UMP is not surprising since it has been shown that the Rv1712 locus in *M. tuberculosis* codes for a functional cytosine monophosphate kinase that preferentially phosphorylates CMP and dCMP, and that UMP is a poor substrate [45]. In agreement with these results, *E. coli* has two distinct enzymes that display substrate specificity for UMP (UMPK) or CMP (CMP kinase) [46]. Steady-state kinetics and ITC data suggest a sequential ordered mechanism for substrate addition to *Mt*UMPK, in which ATP binds first to free enzyme followed by UMP binding; and a random order for release of products.

The cooperative kinetics with respect to ATP, activation by GTP, and inhibition by UTP, showed that *Mt*UMPK is an allosteric enzyme that is subject to a complex control by these metabolites. The results here described also show that *Mt*UMPK belongs to the *K* system. This term was originally proposed by Monod *et al*. [47], in which the enzyme exists at equilibrium between two states with the same catalytic activities, but different substrate affinities (T of low affinity, and R of high affinity). In the absence of effectors, ATP has a positive heterotropic effect on UMP binding to *Mt*UMPK to form the catalytically competent ternary complex. This degree of cooperativity is decreased in the presence of GTP as there is a lowering of the Hill coefficient value, and a decrease in $K_{0.5}$ value for ATP, thereby suggesting increased ATP affinity for *Mt*UMPK. This model may also be applicable to UTP inhibition, in which binding of UTP displaces the equilibrium for the state with lower affinity for ATP with no effect on the Hill coefficient and maximum velocity. Moreover, as UTP is an uncompetitive inhibitor towards UMP, it appears that UTP can have a dual inhibitory effect on *Mt*UMPK enzyme activity depending on which substrate is varied. The results on

*Mt*UMPK mode of action show that its cooperativity is more pronounced than that observed for other UMPKs (*n* values of 1.28-2.5) [19,21,43]. In general, the Hill coefficient does not represent the actual number of sites, unless the cooperativity is high [35]. Our findings show that the *n* value of ATP (3.9) for tetrameric *Mt*UMPK indicates strong positive cooperativity and it may correspond to the actual number of protomers. Activation of *Mt*UMPK by GTP and feedback inhibition by UTP imply a role for this enzyme in coordinating the synthesis of purine v*ersus* pyrimidine nucleoside triphosphates, and highlights the likely relevance of UMPK in the metabolism of *M. tuberculosis*.

The currently available repertoire of antimycobacterial agents reveals only a handful of comprehensively validated targets, namely RNA polymerase, DNA gyrase, NADH-dependent enoyl-ACP reductase and ATP synthase [48]. The complete genome sequencing of *M. tuberculosis* H37Rv strain has accelerated the study and validation of molecular targets aiming at the rational design of anti-TB drugs [23]. The target-based rational design of new agents with anti-TB activity includes functional and structural efforts. However, the first step to enzyme target validation must include experimental data demonstrating that a gene predicted by *in silico* analysis to encode a particular protein catalyzes the proposed chemical reaction. Moreover, it has recently been pointed out that recognition of the limitations of high-throughput screening approaches in the discovery of candidate drugs has rekindled interest in rational design methods [8].Understanding the mode of action of *Mt*UMPK will inform us on how to better design inhibitors targeting this enzyme with potential therapeutic application in TB chemotherapy. Accordingly, it is hoped that the results here described may be useful to the rational design of anti-TB agents and that they may contribute to our understanding of the biology of *M. tuberculosis*.

References

[1] C. Dye, S. Scheele, P. Dolin, V. Pathania, M.C. Raviglione, Global burden of tuberculosis: estimated incidence, prevalence, and mortality by country. J. Am. Med. Assoc. 282 (1999) 677-686.

[2] World Health Organization, Global Tuberculosis Control: a short update to the 2009 report, (2010).

[3] W.W. Yew, C.C. Leung, Management of multidrug-resistant tuberculosis: Update 2007, Respirology. 13 (2008) 21-46.

[4] A.A. Velayati, P. Farnia, M.R. Masjedi, T.A. Ibrahim, P. Tabarsi, R.Z. Haroun, H.O. Kuan, J. Ghanavi, P. Farnia, M. Varahram, Totally drug-resistant tuberculosis strains: evidence of adaptation at the cellular level. Eur. Respir. J. 34 (2009) 1202-1203.

[5] R.G. Ducati, L.A. Basso, D.S. Santos, Mycobacterial shikimate pathway enzymes as targets for drug design, Curr. Drug Targets. 8 (2007) 423-435.

[6] J.G. Robertson, Mechanistic basis of enzyme-targeted drugs, Biochemistry. 44 (2005) 5561-5571.

[7] J.G. Robertson, Enzymes as a special class of therapeutic target: clinical drugs and modes of action. Curr. Opin. Struct. Biol. 17 (2007) 674-679.

[8] J.E. Ladbury, G.K. Klebe, E. Freire, Adding calorimetric data to decision making in lead discovery: a hot tip. Nat. Rev. Drug Discov. 9 (2010) 23-27.

[9] C. Meier, L.G. Carter, S. Sainsbury, E.J. Mancini, R.J. Owens, D.I. Stuart, R.M. Esnouf, The crystal structure of UMP kinase from *Bacillus anthracis* (BA1797) reveals an allosteric nucleotide-binding site, J. Mol. Biol. 381 (2008) 1098-1105.

[10] G.E. Shambaugh, Pyrimidine biosynthesis, Am. J. Clin. Nutr. 32 (1979) 1290-1297.

[11] C. Marco-Marín, F. Gil-Ortiz, V. Rubio, The crystal structure of *Pyrococcus furiosus* UMP kinase provides insight into catalysis and regulation in microbial pyrimidine nucleotide biosynthesis, J. Mol. Biol. 352 (2005) 438-454.

[12] H. Yan, M.D. Tsai, Nucleoside monophosphate kinases: structure, mechanism, and substrate specificity, Adv. Enzymol. Relat. Areas Mol. Biol. 73 (1999) 103-134.

[13] P. Briozzo, C. Evrin, P. Meyer, L. Assairi, N. Joly, O. Barzu, A. Gilles, Structure of *Escherichia coli* UMP kinase differs from that of other nucleoside monophosphate kinases and sheds new light on enzyme regulation, J. Biol. Chem. 280 (2005) 25533-25540.

[14] H.J. Müller-Dieckmann, G.E. Schulz, The structure of uridylate kinase with its substrates, showing the transition state geometry, J. Mol. Biol. 236 (1994) 361-367.

[15] J. Liou, G.E. Dutschman, W. Lam, Z. Jiang, Y. Cheng, Characterization of human

UMP/CMP kinase and its phosphorylation of D- and L-form deoxycytidine analogue monophosphates, Cancer Res. 62 (2002) 1624-1631.

[16] K. Scheffzek, W. Kliche, L. Wiesmüller, J. Reinstein, Crystal structure of the complex of UMP/CMP kinase from *Dictyostelium discoideum* and the bisubstrate inhibitor P1-(5'-adenosyl) P5-(5'-uridyl) pentaphosphate (UP5A) and Mg2+ at 2.2 A: implications for water-mediated specificity, Biochemistry. 35 (1996) 9716-9727.

[17] L. Serina, C. Blondin, E. Krin, O. Sismeiro, A. Danchin, H. Sakamoto, A.M. Gilles, O. Bârzu, *Escherichia coli* UMP-kinase, a member of the aspartokinase family, is a hexamer regulated by guanine nucleotides and UTP, Biochemistry. 34 (1995) 5066-5074.

[18] C. Gagyi, N. Bucurenci, O. Sîrbu, G. Labesse, M. Ionescu, A. Ofiteru, L. Assairi, S. Landais, A. Danchin, O. Bârzu, A. Gilles, UMP kinase from the Gram-positive bacterium *Bacillus subtilis* is strongly dependent on GTP for optimal activity, Eur. J. Biochem. 270 (2003) 3196-3204.

[19] F. Fassy, O. Krebs, M. Lowinski, P. Ferrari, J. Winter, V. Collard-Dutilleul, K. Salahbey Hocini, UMP kinase from *Streptococcus pneumoniae*: evidence for co-operative ATP binding and allosteric regulation, Biochem. J. 384 (2004) 619-627.

[20] K.S. Jensen, E. Johansson, K.F. Jensen, Structural and enzymatic investigation of the *Sulfolobus solfataricus* uridylate kinase shows competitive UTP inhibition and the lack of GTP stimulation, Biochemistry. 46 (2007) 2745-2757.

[21] L. Egeblad-Welin, M. Welin, L. Wang, S. Eriksson, Structural and functional investigations of *Ureaplasma parvum* UMP kinase - a potential antibacterial drug target, FEBS J. 274 (2007) 6403-6414.

[22] K.A. Kantardjieff, C. Vasquez, P. Castro, N.M. Warfel, B.S. Rho, T. Lekin, C.Y. Kim, B.W. Segelke, T.C. Terwilliger, B. Rupp, Structure of pyrR (Rv1379) from *Mycobacterium tuberculosis*: a persistence gene and protein drug target, Acta Crystallogr. D Biol. Crystallogr. 61 (2005) 355-364.

[23] S.T. Cole, R. Brosch, J. Parkhill, T. Garnier, C. Churcher, D. Harris, S.V. Gordon, K. Eiglmeier, S. Gas, C.E. Barry, F. Tekaia, K. Badcock, D. Basham, D. Brown, T. Chillingworth, R. Connor, R. Davies, K. Devlin, T. Feltwell, S. Gentles, N. Hamlin, S. Holroyd, T. Hornsby, K. Jagels, A. Krogh, J. McLean, S. Moule, L. Murphy, K. Oliver, J. Osborne, M.A. Quail, M.A. Rajandream, J. Rogers, S. Rutter, K. Seeger, J. Skelton, R. Squares, S. Squares, J.E. Sulston, K. Taylor, S. Whitehead, B.G. Barrell, Deciphering the biology of *Mycobacterium tuberculosis* from the complete genome sequence, Nature. 393 (1998) 537-544.

[24] D. Robertson, P. Carroll, T. Parish, Rapid recombination screening to test gene essentiality demonstrates that *pyrH* is essential in *Mycobacterium tuberculosis*, Tuberculosis. 87 (2007) 450-458.

[25] K. Yamanaka, T. Ogura, H. Niki, S. Hiraga, Identification and characterization of the *smbA* gene, a suppressor of the *mukB* null mutant of *Escherichia coli*, J. Bacteriol. 174

(1992) 7517-7526.

[26] J.C. Smallshaw, R.A. Kelln, Cloning, nucleotide sequence and expression of the *Escherichia coli* K-12 *pyrH* gene encoding UMP kinase, Genetics (Life Sci. Adv.) 11 (1992) 59-65.

[27] J. Sambrook, D.W. Russel, Molecular Cloning: a Laboratory Manual, Spring Harbor Laboratory Press, New York, 2001.

[28] U.K. Laemmli, Cleavage of structural proteins during the assembly of the head of bacteriophage T4, Nature. 227 (1970) 680-685.

[29] M.M. Bradford, A rapid and sensitive method for the quantitation of microgram quantities of protein utilizing the principle of protein-dye binding, Anal. Biochem. 72 (1976) 248–254.

[30] B. Monson de Souza, M.S. Palma, Monitoring the positioning of short polycationic peptides in model lipid bilayers by combining hydrogen/deuterium exchange and electrospray ionization mass spectrometry, Biochim. Biophys. Acta. 1778 (2008) 2797-2805.

[31] H. Chassaigne, R. Lobinski, Characterization of horse kidney metallothionein isoforms by electrospray MS and reversed-phase HPLC-electrospray MS, Analyst. 123 (1998) 2125-2130.

[32] D.A. Benson, I. Karsch-Mizrachi, D.J. Lipman, J. Ostell, E.W. Sayers, GenBank: update, Nucleic Acids Res. 37 (2009) D26-31.

[32] J.D. Thompson, D.G. Higgins, T.J. Gibson, CLUSTAL W: improving the sensitivity of progressive multiple sequence alignment through sequence weighting, position-specific gap penalties and weight matrix choice, Nucleic Acids Res. 22 (1994) 4673-4680.

[34] J.S. Oliveira, C.A. Pinto, L.A. Basso, D.S. Santos, Cloning and overexpression in soluble form of functional shikimate kinase and 5-enolpyruvylshikimate 3-phosphate synthase enzymes from *Mycobacterium tuberculosis*, Protein Expr. Purif. 22 (2001) 430-435.

[35] I. Segel, Enzyme Kinetics, Behavior and Analysis of Rapid Equilibrium and Steady-state Enzyme Systems, John Wiley and Sons, New York, 1975.

[36] R.A. Copeland, Evaluation of Enzyme Inhibitors in Drug Discovery, John Wiley and Sons, Inc., New Jersey, 2005.

[37] R.G. Bates, H.B. Hetzer, Dissociation Constant of The Protonated Acid Form of 2-Amino-2-(Hydroxymethyl)1,3-Propanediol [Tris-Hydroxymethyl)-Aminomethane] and Related Thermodynamic Quantities From 0 to 50°, J. Phys. Chem. 65 (1961) 667-671.

[38] H. Fukada, K. Takahashi, Enthalpy and heat capacity changes for the proton dissociation of various buffer components in 0.1 M potassium chloride, Proteins. 33 (1998) 159-166.

[39] M.C. Pinna, A. Salis, M. Monduzzi, B.W. Ninham, Hofmeister series: the hydrolytic activity of *Aspergillus niger* lipase depends on specific anion effects, J. Phys. Chem. B. 109 (2005) 5406-5408.

[40] Y. Zhang, P.S. Cremer, Interactions between macromolecules and ions: The Hofmeister series, Curr. Opin. Chem. Biol. 10 (2006) 658-663.

[41] P. Meyer, C. Evrin, P. Briozzo, N. Joly, O. Bârzu, A. Gilles, Structural and functional characterization of *Escherichia coli* UMP kinase in complex with its allosteric regulator GTP, J. Biol. Chem. 283 (2008) 36011-36018.

[42] L. Serina, N. Bucurenci, A.M. Gilles, W.K. Surewicz, H. Fabian, H.H. Mantsch, M. Takahashi, I. Petrescu, G. Batelier, O. Bârzu, Structural properties of UMP-kinase from *Escherichia coli*: modulation of protein solubility by pH and UTP, Biochemistry 35 (1996) 7003-7011.

[43] C. Evrin, M. Straut, N. Slavova-Azmanova, N. Bucurenci, A. Onu, L. Assairi, M. Ionescu, N. Palibroda, O. Bârzu, A. Gilles, Regulatory mechanisms differ in UMP kinases from Gram-negative and Gram-positive bacteria, J. Biol. Chem. 282 (2007) 7242-7253.

[44] S.E. Lee, S.Y. Kim, C.M. Kim, M. Kim, Y.R. Kim, K. Jeong, H. Ryu, Y.S. Lee, S.S. Chung, H.E. Choy, J.H. Rhee, The *pyrH* gene of *Vibrio vulnificus* is an essential *in vivo* survival factor, Infect. Immun. 75 (2007) 2795-2801.

[45] C. Thum, C.Z. Schneider, M.S. Palma, D.S. Santos, L.A. Basso, The Rv1712 Locus from *Mycobacterium tuberculosis* H37Rv codes for a functional CMP kinase that preferentially phosphorylates dCMP, J. Bacteriol. 191 (2009) 2884-2887.

[46] N. Bucurenci, H. Sakamoto, P. Briozzo, N. Palibroda, L. Serina, R.S. Sarfati, G. Labesse, G. Briand, A. Danchin, O. Bărzu, A.M. Gilles, CMP kinase from *Escherichia coli* is structurally related to other nucleoside monophosphate kinases, J. Biol. Chem. 271 (1996) 2856-2862.

[47] J. Monod, J. Wyman, J.P. Changeux, On the Nature of Allosteric Transitions: A Plausible Model, J. Mol. Biol. 12 (1965) 88-118.

[48] T.S. Balganesh, P.M. Alzari, S.T. Cole, Rising standards for tuberculosis drug development, Trends Pharmacol. Sci. 29 (2008) 576-581.

Figure legends

Fig. 1. Chemical reaction catalyzed by UMPK.

Fig. 2. (**A**) 12% SDS-PAGE analysis of total soluble proteins. Expression of *Mt*UMPK of 24-h cell growth after reaching an $OD_{600\ nm}$ of 0.4 - 0.6 in TB medium without addition of IPTG. Lane 1, Protein Molecular Weight Marker (Fermentas); lane 2, soluble *E. coli* BL21 (DE3) [pET-23a(+) (control)] extract; lane 3, soluble *E. coli* BL21 (DE3) [pET-23a(+)::*pyrH*] extract. (**B**) 12% SDS-PAGE analysis of pooled fractions from *Mt*UMPK purification steps. Lane 1, Protein Molecular Weight Marker (Fermentas); lane 2, crude extract; lane 3, HiPrep Q XL 16/10 elution; lane 4, Butyl Sepharose HP elution and Mono Q 16/10 elution.

Fig. 3. Amino acids sequence alignment of UMPKs from eight prokaryotes. The residues inferred in *E. coli* as interacting with ATP, UMP or UDP are shaded in *gray* and the residues involved in GTP-binding are boxed [13,41]. (*), (:), (.) and (-) indicate identity, strong similarity, weak similarity and gat inclusion among the residues, respectively. Amino acid residues were numbered after removing 29 N-terminal amino acids from the polypeptide sequence of *Mt*UMPK.

Fig. 4. Apparent steady-state kinetic parameters. (**A**) Specific activity (U mg^{-1}) *versus* [UMP] (μM) at fixed concentration of ATP (3000 μM). (**B**) Specific activity (U mg^{-1}) *versus* [ATP] (μM) at fixed concentration of UMP (600 μM). The *Mt*UMPK concentration was 70 nM on both assays.

Fig. 5. Double-reciprocal plot of specific activity^{-1} (mg U^{-1}) *versus* [UMP]$^{-1}$ (μM^{-1}) at 0, 30, 50 and 70 μM UTP. The *Mt*UMPK concentration was 80 nM.

Fig. 6. Effect of GTP (500 μM) on ATP saturation curves. In the absence of effector (•), the curve is sigmoidal. In the presence of effector (♦), the sigmoidicity is reduced though still present. The *Mt*UMPK concentration was 70 nM.

Fig. 7. Isothermal titration calorimetric curves of binding of ligands to *Mt*UMPK (100 μM). (**A**) Titration of the ATP at a final concentration of 248 μM. (**B**) Titration of the ADP product at a final concentration of 248 μM. (**C**) Titration of the UDP product at a final concentration of 398 μM. (**D**) Titration of the allosteric effector GTP at a final concentration of 248 μM. The experiments were carried out at constant temperature and pressure.

Fig. 8. Proposed kinetic mechanism for *Mt*UMPK.

Figures

Figure 1.

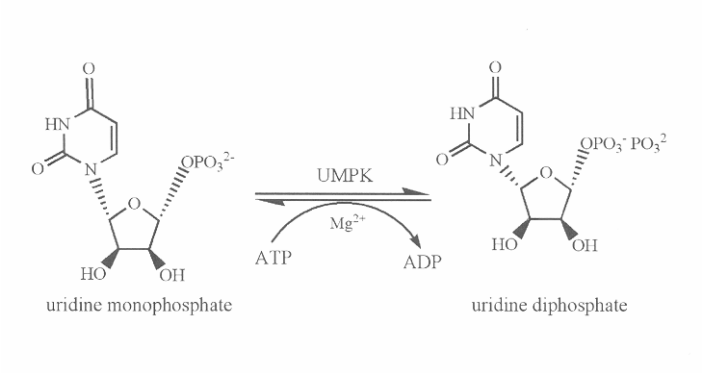

Figure 2.

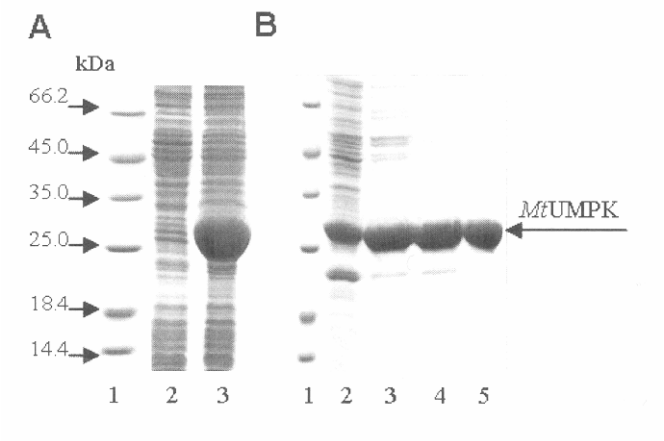

Figure 3.

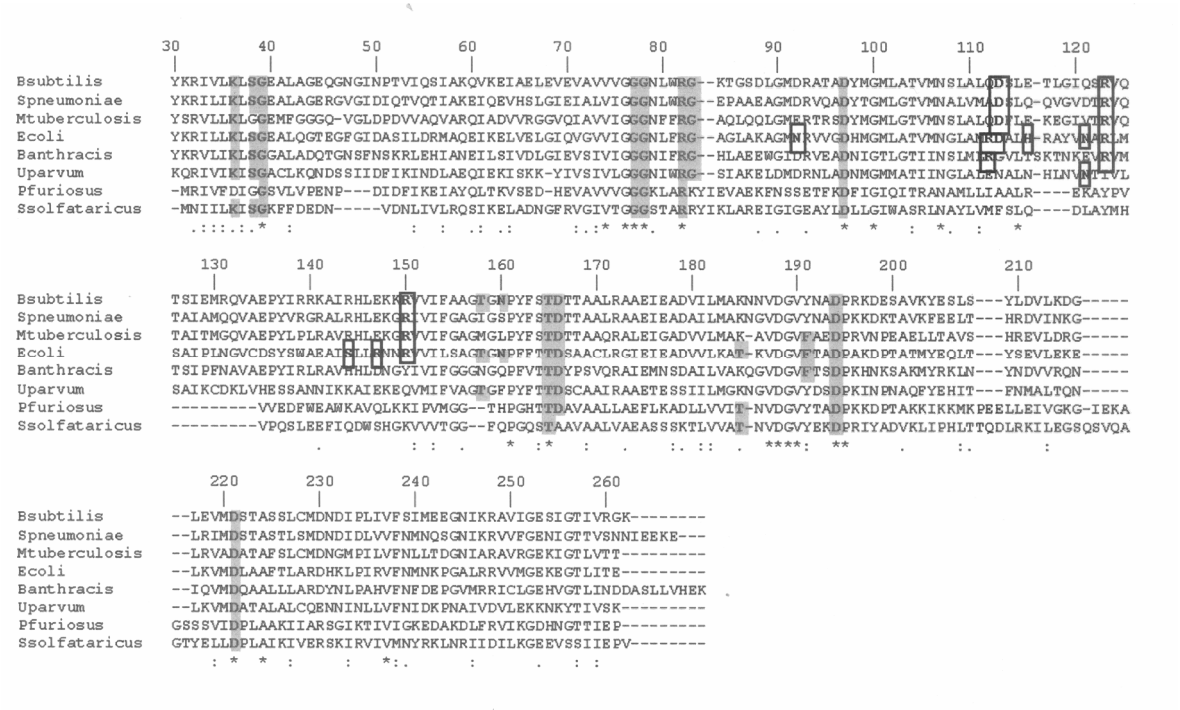
Bsubtilis
Spneumoniae
Mtuberculosis
Ecoli
Banthracis
Uparvum
Pfuriosus
Ssolfataricus

Figure 4.

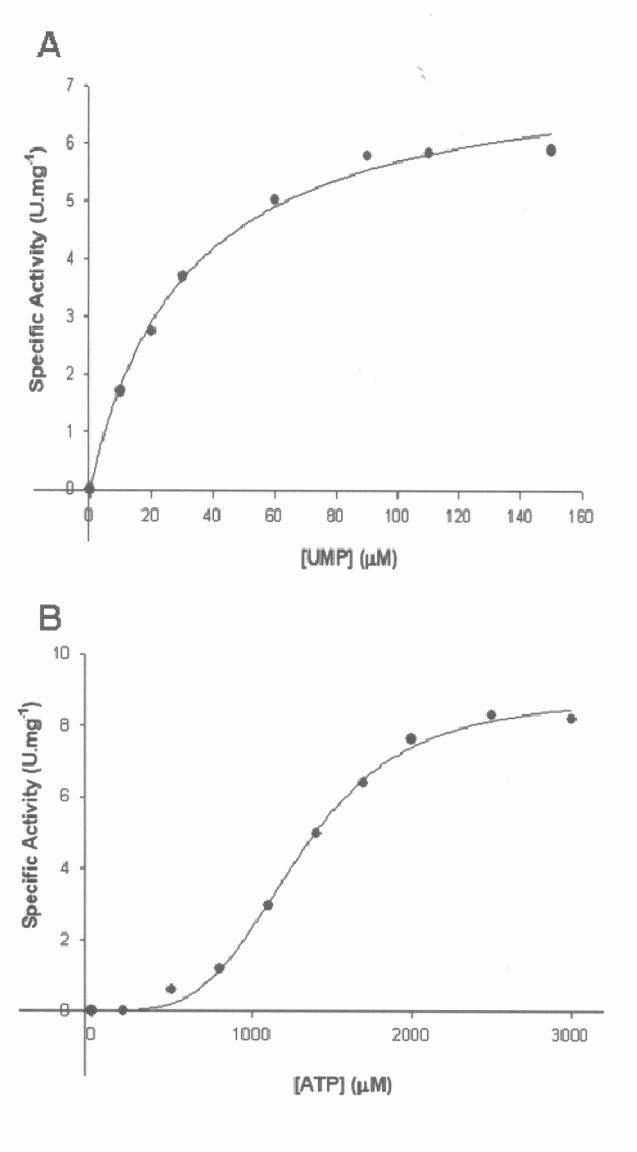
A
Specific Activity (U.mg-1)
0
1
2
3
4
5
6
7
0
20
40
60
80
100
120
140
160
[UMP] (µM)
B
Specific Activity (U.mg-1)
0
2
4
6
8
10
0
1000
2000
3000
[ATP] (µM)

Figure 5.

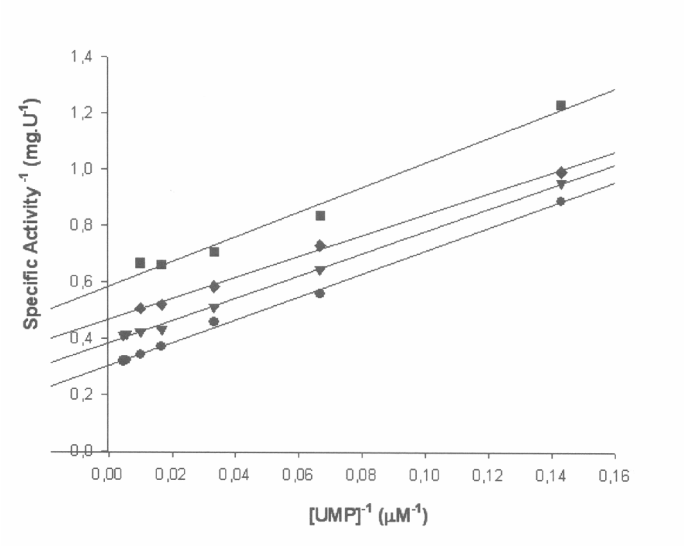

Figure 6.

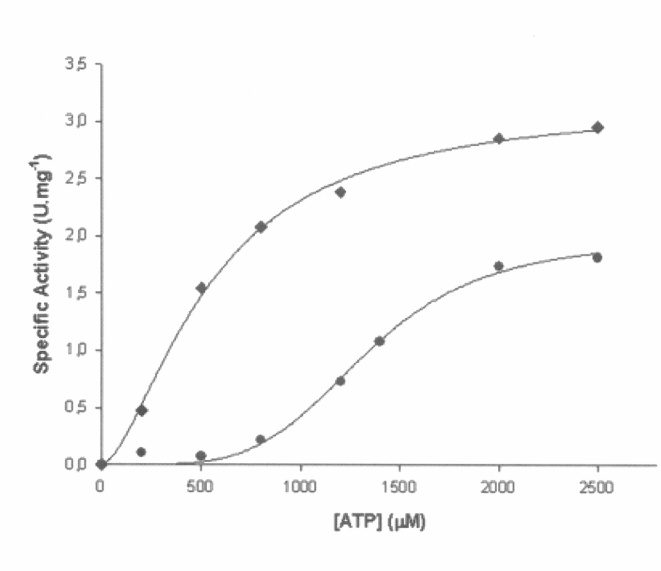

Figure 7.

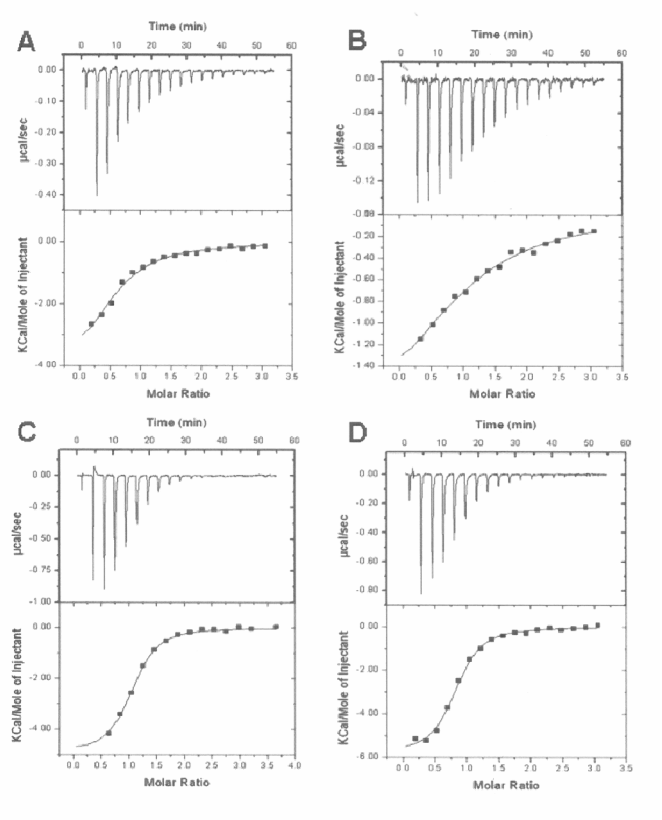

Figure 8.

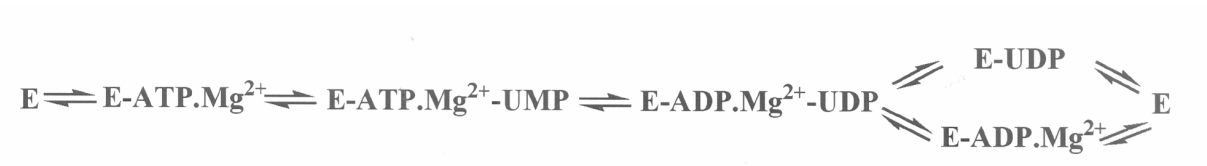

Tables

Table 1

Purification of *Mt*UMPK from *E. coli* BL21 (DE3). Typical purification protocol from 2 g wet cell paste.

Purification step	Total protein (mg)	Total enzyme activity (U)	Specific activity (U mg^{-1})	Purification fold	Yield (%)
Crude extract	158	722.06	4.57	1.0	100
HiPrep Q XL	54.8	977.08	17.83	3.9	135
Butyl Sepharose	27	862.92	31.96	7.0	120
Mono Q	20	153.40	7.67	1.7	21

Table 2

I_{50} and n values for UTP in the presence of different fixed substrate concentrations.

Substrate concentrations	I_{50} (μM)[a]	n[b]
ATP 1300 μM + UMP 600 μM	79.6 ± 4.3	1.5 ± 0.1
ATP 1300 μM + UMP 30 μM	97.2 ± 6.5	2.8 ± 0.4
ATP 3000 μM + UMP 30 μM	209.6 ± 5.9	3.6 ± 0.3

[a] I_{50} = concentration of inhibitor required to half-saturate the enzyme population.

[b] n = the Hill coefficient.

Table 3

Association constants and thermodynamic parameters of different ligands binding to *Mt*UMPK.

Ligands	n[a]	K_a[b] (M^{-1})	$\Delta H°$[c] (kcal.mol^{-1})	$\Delta G°$[d] (kcal.mol^{-1})	$\Delta S°$[e] (cal.mol^{-1}.K^{-1})	K_d[f] (μM)
ATP	0.57	3.05e^4	-4.82	-6.11	4.35	32.8
ADP	1.06	1.54e^4	-2.11	-5.71	12.1	64.9
UDP	1.01	2.11e^5	-4.90	-7.26	7.92	4.7
GTP	0.79	2.00e^5	-5.84	-7.23	4.66	5.0

[a] n = number of sites. [b]K_a = association constant. [c]$\Delta H°$ = binding enthalpy.

[d]$\Delta G°$ = Gibbs free energy. [e]$\Delta S°$ = binding entropy. [f]K_d = dissociation constant.

6. CONSIDERAÇÕES FINAIS

A pesquisa e o desenvolvimento de compostos mais efetivos contra a TB representam uma urgente necessidade à saúde pública mundial. Embora isso envolva políticas governamentais, financiamento e transferência de tecnologia, um melhor entendimento sobre a biologia molecular do bacilo é indispensável para que futuros tratamentos sejam mais efetivos na prevenção e combate à doença.

Nesse contexto, as rotas metabólicas envolvidas em processos bioquímicos essenciais à viabilidade do bacilo compartilham inúmeros alvos potenciais para drogas. Enzimas indispensáveis para a sobrevivência do bacilo e que são ausentes ou não se assemelham às enzimas presente em humanos, são alvos promissores para o desenho racional de inibidores. A importância da caracterização da enzima *Mt*UMPK advém do fato dela preencher os requisitos de toxicidade seletiva.

Durante este trabalho foi realizada a amplificação do gene *pyrH* e, através de expressão da proteína recombinante em *E. coli* e purificação através de três etapas cromatográficas, foi possível determinar que o produto do gene *pyrH* corresponde a uma enzima funcional que catalisa a fosforilação de UMP a UDP. Além disso, a determinação de sua massa molecular, bem como o seqüenciamento dos 22 primeiros aminoácidos, corroboraram a identidade da proteína. Estudos de cinética enzimática indicaram que a *Mt*UMPK é uma enzima alostérica, ativada por GTP e inibida por UTP. Através da técnica de ITC, foram determinados os parâmetros termodinâmicos envolvidos na ligação da enzima a seus substratos, produtos e efetor alostérico GTP. Além disso, demonstrou-se que o mecanismo cinético é sequencial ordenado, onde a formação do complexo ternário ocorre pela ligação da molécula de ATP na enzima livre seguido da ligação do UMP, e que a dissociação dos produtos ocorre aleatoriamente.

Este trabalho resultou na caracterização da enzima *Mt*UMPK como alvo para inibidores. Futuros estudos bioquímicos e estruturais serão realizados, a fim de avaliar possíveis moléculas inibidoras que possam ser testadas no tratamento da TB.

REFERÊNCIAS

1. Disponível em: <http://www.who.int/topics/tuberculosis/en/>. Acesso em: junho de 2010.

2. Palomino JC, Leão SC, Ritacco V. Tuberculosis 2007 - From basic science to patient care. Disponível em: <www.TuberculosisTextbook.com>. Acesso em: maio de 2010.

3. Ducati RG, Ruffino-Neto A, Basso LA, Santos DS. The resumption of consumption – A review on tuberculosis. Ment Inst Oswaldo Cruz. 2006;101:697-714.

4. Bloom BR, Murray CJL. Tuberculosis: Commentary on a Reemergent Killer. Science. 1992;257:1055-1064.

5. Jarlier V, Nikaido H. Mycobacterial cell wall: Structure and role in natural resistance to antibiotics. FEMS Microbiol Lett. 1994;123:11-18.

6. World Health Organization. Global Tuberculosis Control: a short update to the 2009 report. WHO, Geneva 2010.

7. World Health Organization. Treatment of tuberculosis: guidelines for national programmes. WHO, Geneva, 2003.

8. Flynn JL, Chan J. Immunology of Tuberculosis. Annu Rev Immunol. 2001;19:93-129.

9. Elston JWT, Thaker HKB. Co-infection with human immunodeficiency virus and tuberculosis. Indian J Dermatol Venereol Leprol. 2008;74:194-198.

10. Russel DG. Who puts the tubercle in tuberculosis? Nat Rev Microbiol. 2007;5:39-47.

11. Ramaswamy S, Musser JM. Molecular genetics basis of antimicrobial agent resistance in *Mycobacterium tuberculosis*: 1998 update. Tuber Lung Dis. 1998;79:3-29.

12. Yew WW, Leung CC. Management of multidrug-resistant tuberculosis: Update 2007. Respirology. 2008;13:21-46.

13. Zager EM, McNerney R. Multidrug-resistant tuberculosis. BMC Infect Dis. 2008;8:1-5.

14. Dorman SE, Chaisson RE. From magic bullets back to the Magic Mountain: the rise of extensively drug-resistant tuberculosis. Nature Medicine. 2007;13:295-298.

15. World Health Organization. Multidrug and extensively drug-resistant TB (M/XDR-TB): 2010 global report on surveillance and response. WHO, Geneva 2010.

16. Centers for Disease Control and Prevention. Emergence of *Mycobacterium tuberculosis* with extensive resistance to second-line drugs - worldwide, 2000-2004. MMWR Morb Mortal Wkly Rep. 2006;55:301-305.

17. Kawai V, Soto G, Gilman RH, Bautista CT, Caviedes L, Huaroto L, et al. Tuberculosis mortality, drug resistance, and infectiousness in patients with and without HIV infection in Peru. Am J Trop Med Hyg. 2006;75:1027-1033.

18. Jassal M, Bishai WR. Extensively drug-resistant tuberculosis. Lancet Infect Dis. 2008. Epub 2008 Nov 5.

19. Gandhi NR, Moll A, Sturm AW, Pawinski R, Govender T, Lalloo U, et al. Extensively drug-resistant tuberculosis as a cause of death in patients co-infected with tuberculosis and HIV in a rural area of South Africa. Lancet. 2006;386:1575-1580.

20. Velayati AA, Masjedi MR, Farnia P, Tabarsi P, Ghanavi J, ZiaZarifi AH, Hoffner SE. Emergence of New Forms of Totally Drug-Resistant Tuberculosis Bacilli. CHEST. 2009;136:420-425.

21. Balganesh TS, Alzari PM, Cole ST. Rising standards for tuberculosis drug development. Trends Pharmacol Sci. 2008;29:576-581.

22. O´Brien RJ, Nunn PP. The need for new drugs against tuberculosis. Am J Respir Crit Care Med. 2001;162:1055-1058.

23. Souza MVN. Promising drugs against tuberculosis. Recent Pat Antiinfect Drug Discov. 2006;1:33-44.

24. Voet D, Voet JG. Bioquímica. 3ª ed. Porto Alegre: Artmed Editora S.A.; 2006.

25. Smith C, Marks AD, Lieberman M. Marks´ Basic Medical Biochemistry - A Clinical Approach. 2nd ed. U.S.A: Lippincott Williams & Wilkins; 2005.

26. Nelson DL, Cox MM. Lehninger - Principles of Biochemistry. 4th ed. New York: W.H. Freeman and Company; 2005.

27. Shambaugh GE. Pyrimidine biosynthesis. Am J Clin Nutr. 1979;32:1290-1297.

28. Connolly GP, Duley JA. Uridine and its nucleotides: biological actions, therapeutic potentials. TiPS. 1999;20:218-225.

29. Turnbough Jr CL, Switzer RL. Regulation of Pyrimidine Biosynthetic Gene Expression in Bacteria: Repression without Repressors. Microbiol Mol Biol Ver. 2008;72:266-300.

30. Yan H, Tsai MD. Nucleoside Monophosphate Kinases: Structure, Mechanism, and Substrate Specificity. Adv Enzymol Relat Areas Mol Biol. 1999;73:103-131.

31. Briozzo P, Evrin C, Meyer P, Assairi L, Joly N, Bârzu O, et al. Structure of *Escherichia coli* UMP Kinase Differs from That of Other Nucleoside Monophosphate Kinases and Sheds New Light on Enzyme Regulation. J Biol Chem. 2005;280:25533-25540.

32. Müller-Dieckmann HJ, Schulz GE. The structure of Urydilate Kinase with Its Substrates, Showing the Transition State Geometry. J Mol Biol. 1994;236:361-367.

33. Liou J, Dutschman DE, Lam W, Jiang Z, Cheng Y. Characterization of human UMP/CMP kinase and its phosphorylation of D- and L-form deoxycytidine analogue monophosphates. Cancer Res. 2002;62:1624-1631.

34. Scheffzek K, Kliche W, Wiesmüller L, Reinstein J. Crystal Structure of the Complex of UMP/CMP Kinase from *Dictyostelium discoideum* and the Bisubstrate Inhibitor P^1-(5´-Adenosyl) P^5-(5´-Uridyl) Pentaphosphate (UP_5A) and Mg^{2+} at 2.2 A: Implications for Water-Mediated Specificity. Biochemistry. 1996;35:9716-9727.

35. Bucurenci N, Sakamoto H, Briozzo P, Palibroda N, Serina L, Sarfati RS, et al. CMP Kinase from *Escherichia coli* Is Structurally Related to Other Nucleoside Monophosphate Kinases. J Biol Chem. 1996;271:2856-2862.

36. Gagyi C, Bucurenci N, Sîrbu O, Labesse G, Ionescu M, Ofiteru A, et al. UMP kinase from the Gram-positive bacterium *Bacillus subtilis* is strongly dependent on GTP for optimal activity. Eur J Biochem. 2003;270:3196-3204.

37. Labesse G, Bucurenci N, Douguet D, Sakamoto H, Landais S, Gagyi C, et al. Comparative modelling and immunochemical reactivity of *Escherichia coli* UMP kinase. Biochem Biophys Res Commun. 2002;294:173-179.

38. Marco-Marín C, Gil-Ortiz F, Rubio V. The Crystal Structure of *Pyrococcus furiosus* UMP Kinase Provide Insight into Catalysis and Regulation in Microbial Pyrimidine Nucleotide Biosynthesis. J Mol Biol. 2005;352:438-454.

39. Serina L, Blondin C, Krin E, Sismeiro O, Danchin A, Sakamoto H, et al. *Escherichia coli* UMP-Kinase, a Member of Aspartokinase Family, Is a Hexamer Regulated by Guanine Nucleotides and UTP. Biochemistry. 1995;34:5066-5074.

40. Fassy F, Krebs O, Lowinski M, Ferrari P, Winter J, Collard-Dutilleul V, et al. UMP kinase from *Streptococcus pneumoniae*: evidence for co-operative ATP binding and allosteric regulation. Biochem J. 2004;384:619-627.

41. Yamanaka K, Ogura T, Niki H, Hiraga S. Identification and characterization of the *smbA* gene, a suppressor of the *mukB* null mutant of *Escherichia coli*. J Bacteriol. 1992;174:7517-7526.

42. Smallshaw JC, Kelln RA. Cloning, nucleotide sequence and expression of the *Escherichia coli* K-12 *pyrH* gene encoding UMP kinase. Genetics. 1992;11:59-65.

43. Kobayashi K, Ehrlich SD, Albertini A, Amati G, Andersen KK, Arnaud M, et al. Essential *Bacillus subtilis* genes. Proc Natl Acad Sci U.S.A. 2003;100:4678-4683.

44. Ducati RG, Basso LA, Santos DS. Mycobacterial shikimate pathway enzymes as targets for drug design. Curr Drug Targets. 2007;8:423-435.

45. Robertson D, Carroll P, Parish T. Rapid recombination screening to test gene essentiality demonstrates that *pyrH* is essential in *Mycobacterium tuberculosis*. Tuberculosis. 2007;87:450-458.

46. Disponível em: <http://genolist.pasteur.fr/TubercuList/>. Acesso em: julho de 2008.

47. Benson DA, Karsch-Mizrachi I, Lipman DJ, Ostell J, Sayers EW. GenBank: update. Nucleic Acids Res. 2009;37:D26-31.

48. Thompson JD, Higgins DG, Gibson TJ. CLUSTAL W: improving the sensitivity of progressive multiple sequence alignment through sequence weighting, position-specific gap penalties and weight matrix choice. Nucleic Acids Res. 1994;22:4673-4680.

49. Serina L, Bucurenci N, Gilles AM, Surewicz WK, Fabian H, Mantsch HH, et al. Structural Properties of UMP-Kinase from *Escherichia coli*: Modulation of Protein Solubility by pH and UTP. Biochemistry. 1996;35:7003-7011.